
Recommendations for best practice for iron speciation by competitive ligand exchange adsorptive cathodic stripping voltammetry with salicylaldoxime

Mahieu Léo ^{1,2,*}, Omanović Dario ³, Whitby Hannah ¹, Buck Kristen N. ^{2,4}, Caprara Salvatore ⁴, Salaün Pascal ¹

¹ Ocean Sciences, School of Environmental Sciences, University of Liverpool, Liverpool L69 3GP, UK

² College of Earth, Ocean and Atmospheric Sciences, Oregon State University, Corvallis, OR 97333, USA

³ Ruđer Bošković Institute, Division for Marine and Environmental Research, 10002 Zagreb, Croatia

⁴ College of Marine Science, University of South Florida, Saint Petersburg, FL 33701, USA

* Corresponding author : Léo Mahieu, email address : leo.mahieu@oregonstate.edu

Abstract :

The method of competitive ligand exchange followed by adsorptive cathodic stripping voltammetry (CLE-AdCSV) allows for the determination of dissolved iron (DFe) organic speciation parameters, i.e., ligand concentration (LFe) and conditional stability constant (log K). Investigation of DFe organic speciation by CLE-AdCSV has been conducted in a wide range of marine systems, but aspects of its application pose challenges that have yet to be explicitly addressed. Here, we present a set of observations and recommendations to work toward establishing best practice for DFe organic speciation measurements using the added ligand salicylaldoxime (SA). We detail conditioning procedures to ensure a stable AdCSV signal and discuss the processes at play during conditioning. We also present step-by-step guidelines to simplify CLE-AdCSV data treatment and interpretation using the softwares ECDSOFT and ProMCC and a custom spreadsheet. We validate our application and interpretation methodology with the model siderophore deferoxamine B (DFO-B) in a natural seawater sample. The reproducibility of our application and interpretation methodology was evaluated by running duplicate titrations on 19 samples, many of which had been refrozen prior to the duplicate analysis. Nevertheless, 50% of the duplicate analyses agreed within 10% of their relative standard deviation (RSD), and up to 80% within 25% RSD, for both LFe and log K . Finally, we compared the sequential addition and equilibration of DFe and SA with overnight equilibration after simultaneous addition of DFe and SA on 24 samples. We found a rather good agreement between both procedures, with 60% of samples within 25% RSD for LFe (and 43% of samples for log K), and it was not possible to predict differences in LFe or log K based on the method applied, suggesting specific association/dissociation kinetics for different ligand assemblages. Further investigation of the equilibration kinetics against SA may be helpful as a potential way to distinguish natural ligand assemblages.

Keywords : iron ligands, adsorptive cathodic stripping voltammetry (CLE-AdCSV), salicylaldoxime (SA), conditioning, interpretation, comparison

Introduction

Iron (Fe) is an essential micronutrient for phytoplankton growth (Morel and Price, 2003; Twining and Baines, 2013), limiting primary productivity in up to 40% of open ocean waters (Moore et al., 2013). A fraction of the dissolved organic matter (DOM) is able to bind Fe and enhance its dissolution in seawater above the theoretical solubility limit (Liu and Millero, 2002). This complexation maintains Fe in the dissolved phase (DFe, defined by the porosity of the filter used of 0.2 or 0.45 μm), increasing its residence time in the water column and thus its potential bioavailability. It is thought that more than 99% of DFe is bound to the fraction of the DOM that acts as Fe-binding ligands (FeL; Gledhill and van den Berg, 1994), however, there is still much to learn about ligand composition and biogeochemical cycling (Gledhill and Buck, 2012; Hassler et al., 2017). Multiple studies have focused on aspects of the organic iron ligand pool, from acid-base properties (Lodeiro et al., 2020; Wang et al., 2021) to photodegradation (Barbeau et al., 2001; Hassler et al., 2019), or transformation through remineralisation (Bressac et al., 2019; Whitby et al., 2020a). A considerable number of electrochemical methods have been developed to investigate and identify FeL groups. So far, studies

have helped to define the ability of exopolymeric substances to bind Fe (Hassler et al., 2015, 2011; Norman et al., 2015), and to identify the essential role of the electroactive fraction of humic-like substances (eHS), thought to control DFe distribution in open-ocean deep waters (Whitby et al., 2020b). Other techniques have been compared to electrochemical methods to assess the contribution of ligands such as siderophores (Bundy et al., 2018) or the fluorescent fraction of HS (Heller et al., 2013), but FeL and DFe distribution are not fully resolved despite these efforts (e.g., Bundy et al., 2015; Fourrier et al., 2022; Dulaquais et al., 2023).

The CLE-AdCSV approach

The competitive ligand exchange followed by adsorptive anodic stripping voltammetry (CLE-AdCSV) is classically used to investigate the complexing properties of the FeL fraction. Namely, it allows the determination of the conditional total ligand concentration (L_{Fe} in nmoleqFe L^{-1} ; nMeqFe) and the conditional stability constant (expressed as a logarithmic value and relative to inorganic Fe (Fe^{2+}), $\log K_{Fe/L}^{\text{cond}}$). The CLE-AdCSV approach has been thoroughly explained previously (e.g., Gledhill and van den Berg, 1994; Rue and Bruland, 1995; Abualhaija and van den Berg, 2014; Gerringa et al., 2014; Pižeta et al., 2015). Briefly, its principle is based on the competition for Fe complexation between the natural FeL and an added ligand (AL) of well-characterised ability to bind Fe. This competition is carried out in several aliquots of the sample at increasing DFe concentration resulting in a chemical equilibrium being reached between AL, FeL and DFe. Then, for each aliquot, the FeAL complex is quantified by AdCSV on a hanging mercury drop electrode (HMDE). The measurement consists of an accumulation step, where FeAL adsorbs on the mercury surface, before a stripping step, where adsorbed and bound Fe(III) is reduced to Fe(II). By plotting the intensity of the FeAL reduction peak against total DFe, a titration curve is obtained (total DFe being the sum of naturally present and added DFe). At high DFe concentrations in the titration curve, if natural FeL are saturated, the FeAL signal is considered as linear and proportional to DFe additions while at low DFe, L_{Fe} and AL are competing for DFe (e.g., Figure 2.1 in Mahieu, 2023). There are several methods that can be used to obtain L_{Fe} and $\log K_{Fe/L}^{\text{cond}}$ from the titration curve (Pižeta et al., 2015), but those based on the Langmuir isotherm are the most commonly used, greatly facilitated by user-friendly software such as

ProMCC (Omanović et al., 2015). This software presents the titration curve simultaneously obtained by the Scatchard transformation (Scatchard, 1949), the Ružić/van den Berg linearization (Ružić, 1982; van den Berg, 1982), and the Langmuir/Gerringa transformation (Gerringa et al., 1995, 2014), allowing also the user to overlay the fitted titration curves with the experimental data as a visual tool for results verification. The software ProMCC is commonly applied to the interpretation of metal speciation titrations, and the output from ProMCC includes a 95% confidence interval for the results, although there is currently no established procedure for assigning a titration quality control flag, which would be useful for data management archives.

Added ligand and detection window

There are currently four AL in use to study DFe organic speciation in marine systems: 1-nitroso-2-naphthol (NN; Gledhill and van den Berg, 1994; van den Berg, 1995), 2-(2-thiazolylazo)-p-cresol (TAC; Croot and Johansson, 2000), dihydroxynaphthalene (DHN; van den Berg, 2006; Sanvito and Monticelli, 2020), and salicylaldoxime (SA; Ružić and Bruland, 1995; Buck et al., 2007; Abualhaija and van den Berg, 2014). They all have specific limitations. NN can be used at different pH but suffers from sensitivity issues (Gledhill et al., 2015; Avendaño et al., 2016). It also does not compete with part of the HS-bound DFe pool, resulting in an underestimation of L_{Fe} (Laglera et al., 2011; Ardiningsih et al., 2021), which is a similar problem for the added ligand TAC (Laglera et al., 2011). On the other hand, previous studies have suggested an overestimation of L_{Fe} with SA (Slagter et al., 2019; Gerringa et al., 2021). DHN is not as widely used because of its relatively quick oxidation by oxygen which occurs within the time scale of the equilibration step (Sanvito and Monticelli, 2020).

The AL concentration ($[AL]$; in mol L⁻¹; nM) and its conditional stability constant ($K_{Fe/AL}^{cond}$ or $\beta_{Fe/AL}^{cond}$) defines the detection window of the titration ($\alpha_{FeAL} = [AL]^n \times \beta_{Fe/AL}^{cond}$), often expressed as a logarithmic value ($\log \alpha_{FeAL}$; Table 1). The range of $\log \alpha_{FeAL}$ for which an AL is able to compete with FeL has been estimated to range between 1 to 2 orders of magnitude above and below the calibrated $\log \alpha_{FeAL}$ (Apte et al., 1988; van den Berg and Donat, 1992; Miller and Bruland, 1997; Laglera et al., 2013; Laglera and Filella, 2015). In the case of SA, higher L_{Fe} than those obtained with TAC or NN are

systematically observed (Buck et al., 2016; Slagter et al., 2019; Ardiningsih et al., 2021), possibly due to those latter AL being insensitive to a fraction of weaker Fe-complexing HS (Boye et al., 2001; van den Berg, 2006; Laglera et al., 2011; Ardiningsih et al., 2021; Gerringa et al., 2021), in agreement with the higher detection window corresponding to TAC and NN applications (Table 1).

Table 1. Typical AL concentrations and corresponding detection windows ($\log \alpha_{\text{FeAL}}$) for the different ALs in use to investigate FeL by CLE-AdCSV. $K_{\text{FeAL}}^{\text{cond}}$ and $\beta_{\text{FeAL}}^{\text{cond}}$ used for the calculation of α_{FeAL} can be found in the references given in the Table.

Added ligand	Concentration (μM)	$\log \alpha_{\text{FeAL}}$	Reference and comment
NN	2	2.4	van den Berg (1995)
	7	4	“
	8.7	4.3	“
	15	5	“
TAC	10	2.4	Croot and Johansson (2000)
SA	5	1.2	Abualhaija and van den Berg (2014) considering FeSA and FeSA ₂
	25	1.9	Buck et al. (2007) considering FeSA ₂
DHN	0.5	2.7	Sanvito and Monticelli (2020)
	1	3.2	“
	5	4	“
	10	4.2	“

SA has been used at the basin scale (Buck et al., 2015, 2018), in hydrothermal systems (Kleint et al., 2016), and does not clearly suffer from interference with HS (Laglera et al., 2011; Abualhaija and van den Berg, 2014). There are, however, uncertainties regarding its chemistry and the optimum experimental conditions. Abualhaija and van den Berg (2014) suggested that a non-electroactive FeSA₂ complex slowly forms during the overnight equilibration step when using SA concentrations in the range of 25 μM , which was not experimentally attested; they advised to use a low SA concentration (5 μM) to limit any formation of FeSA₂. Their equilibration procedure consisted of first adding DFe to the aliquot, leave it to equilibrate with the natural ligands for at least 10 min (and not more than 2 hours), followed by addition of 5 μM SA and overnight equilibration (i.e. from 6h to 16h). On the other hand, Rue and Bruland (1995) and Buck et al. (2007) reported a shorter sequential

equilibration procedure: DFe is first added and left to equilibrate with natural ligands for a minimum of 2 h; a relatively high SA concentration (27.5 μM or 25 μM) is then added and left to equilibrate for at least 15 min before starting voltametric analysis. Both these approaches have been applied to the accurate characterization of model ligands (Rue and Bruland, 1995; Buck et al., 2010; Abualhaija and van den Berg, 2014; Bundy et al., 2018). Nevertheless, the two equilibration procedures have not yet been directly compared for determination of L_{Fe} and $\log K_{\text{Fe/L}}^{\text{cond}}$ at similar SA concentration.

Although the FeSA signal has been reported to be stable in the presence of oxygen (Abualhaija and van den Berg, 2014), a decreasing signal has been reported by several authors (Rue and Bruland, 1995; Buck et al., 2007; Ardiningsih et al., 2021; Gerringa et al., 2021). This instability may have various causes, ranging from progressive deoxygenation of the sample (Abualhaija and van den Berg, 2014), stabilization of Fe hydroxides with time (Dulaquais et al., 2023), or the kinetically slow formation of electro-inactive FeSA₂ complexes suggested by Abualhaija and van den Berg (2014). Adsorption is also strongly suspected with SA and conditioning of the voltametric cells and sample vessels prior to speciation measurements is common practice, but has yet to be addressed empirically in the literature (Rue and Bruland, 1995; Buck et al., 2007, 2012; Bundy et al., 2014).

Sample preparation and technical limitations

The quality and reliability of ligand titration results is also dependent on the number of seawater aliquots prepared for the analysis of a sample. It is recommended to run a titration with two aliquots of the sample without metal added and at least 8 aliquots with metal added (for a total of ≥ 10 ; Sander et al., 2011; Gledhill and Buck, 2012), and ideally up to 15 points to maintain a decent analytical time (Omanović et al., 2015; Buck et al., 2016). Analysing two aliquots without added metal helps ensure the validity of the initial point by conditioning the voltametric cell and resolving any carry-over from previous measurements. The concentration range for DFe additions is typically dictated by the amount of L_{Fe} expected in the sample or adjusted to the amount detected (Gledhill and Buck, 2012). The complexation properties obtained from the titration curve heavily depends on the definition of the sensitivity (S) of the method. S is given by the slope of the peak intensity versus DFe when all natural

FeL are saturated in the aliquots amended with high DFe concentrations. Alternatively, the sensitivity can also be fitted, meaning that instead of assuming FeL saturation in the final aliquots, the sensitivity is optimised by iteration to limit the fitting error on the whole titration (Omanović et al., 2015); this can be especially useful for copper speciation, where large pools of weaker ligands are not always titrated (Pižeta et al., 2015). Accurate determination of the sensitivity is still a challenge of the CLE-AdCSV approach (Gerringa et al., 1995, 2014; Omanović et al., 2015; Pižeta et al., 2015). So far, there is no common best practice for its definition for Fe.

The fitting of the data is more challenging when more than one class of FeL is detected. In some cases, and mostly with SA as added ligand, the shapes of the Scatchard and Ružić-van den Berg plots exhibit a kink that suggests the presence of two distinct classes of FeL, whose complexing parameters can be quantified if they are sufficiently separated in $\log K_{FeL}^{cond}$ (Ibisanmi et al., 2011; Gledhill and Buck, 2012; Buck et al., 2015). In order to accurately characterize more than one ligand class in a sample, however, a sufficient number of aliquots must be analysed to allow for the degrees of freedom needed to resolve two ligand groups, which lengthens the analytical time required for each titration (Buck et al., 2012). The results can also be impacted by subjectivity of the analyst when interpreting the titration data. Intercomparison efforts on the interpretation of CLE-AdCSV titrations revealed discrepancies that were partly explained by the choices of the analyst on the selection of the titration datapoints in the case of copper (Pižeta et al., 2015). This problem has not been clearly identified for Fe, but the development of a systematic approach for analyzing titration data applicable to different metals should result in better reproducibility and comparability between laboratories.

In this work, we revisit some of the limiting factors that prevent a wider use and comparability of the SA method for DFe organic speciation. We propose an optimised methodology that spans the conditioning of the voltametric cell and aliquot vessels (here, polypropylene tubes, Metal Free, Labcon™ and perfluoroalkoxy alkane (PFA) vials, Savillex™), the optimisation of voltametric parameters for the detection of the electroactive FeSA complex, and recommendations for data treatment of voltammograms and titrations. We present guidelines for a quick and reliable measurement of the peak-height using the freely available software ECDSOft (Supplementary

Material, SM1). We also developed a step-by-step approach for systematic treatment of titration data, to assess titration quality in a non-subjective manner and improve dataset comparability between users (SM2). Based on the use of the software PromCC with a freely available home-made spreadsheet (SM3), the procedure includes the statistical identification of outliers and the semi-automatic determination of quality flags for the titration data. We also estimated the reproducibility of the sequential addition of Fe and SA with short equilibration time (15 min equilibration; Rue and Bruland, 1995; Buck et al., 2007), and present here a comparison between the speciation parameters (L_{Fe} and $\log K_{Fe/L}^{cond}$) obtained by sequential and shorter equilibration versus overnight equilibration (Abualhaija and van den Berg, 2014; SM4). This work focuses on technical specificities related to the application of the CLE-AdCSV method; for the theoretical aspect of the method, we refer readers to previous work (e.g., Rue and Bruland, 1995; Gledhill and van den Berg, 1994; Abualhaija and van den Berg, 2014; Gerringa et al., 2014; Pižeta et al., 2015).

Method

Apparatuses

MetrohmTM system

The voltametric systems were composed of a 663 VA stand (MetrohmTM) installed in a laminar flow hood (class-100), supplied with nitrogen and equipped with a multi-mode electrode (MME, MetrohmTM) used as hanging mercury drop electrode (HMDE) mounted with a silanized capillary, a glassy carbon counter electrode and a silver/silver chloride reference electrode, all provided by MetrohmTM. Both the counter and reference electrodes were placed in glass bridges filled with 3M KCl. The KCl solution was previously cleaned of organics through UV radiation in quartz tube for 6 h using a home-made UV-digestion apparatus equipped with a 125 W mercury vapour lamp (described here: http://pcwww.liv.ac.uk/~sn35/Site/UV_digestion_apparatus.html), and cleaned of metals with overnight equilibration with manganese oxides (Yokoi and van den Berg, 1992) and filtered through syringe filter (Millex HA, MilliporeTM; Mahieu, 2023). We did not experience interferences from the diffusion of manganese from the KCl placed in the glass bridges, but we advise to use cleaning resins

in future work (e.g., Donat and Bruland, 1988). Voltametric measurements were carried out in 5 mL of oxygenated seawater placed in custom-made PTFE cells which support measurements in small volumes, initially cleaned by successive 1 week-long soaking in DeconTM detergent, 1 M HCl bath, and 0.1 M HCl bath (Gourain, 2020). For each system, a potentiostat/galvanostat μ Autolab III and an IME663 were controlled by the software NOVA 2.5, allowing automatic formation of the drop (size 3) and stirring of the solution through home-made vibrating devices. The home-made stirring device consisted of a small vibration motor (6 mm diameter, 12 mm long, 1.5 V, 10200 rpm, JinLong Machinery, China) connected to a melted pipette with the flat-tip (polypropylene) penetrating the solution. In this instance the use of the home-made stirring device within a smaller voltametric cell, as in Chapman and van den Berg (2007), was favored over the classic polytetrafluoroethylene (PTFE) rods as it enabled working in lower sample volumes, although similar results are obtained with commercialized stirrer and the vibrating devices used here (Mahieu, 2023). To avoid progressive deoxygenation of the sample, the nitrogen blanketed gas flow was stopped by tightening the screw on the left side of the 663 VA stand, and a small aquarium pump (HD-603, HDOMTM) placed inside the laminar flow hood was blowing a stream of air above the water sample to ensure constant dissolved oxygen saturation (Sanvito et al., 2019; Sanvito and Monticelli, 2020; Mahieu, 2023).

The MetrohmTM systems are pressurized with gas and the mercury oxidizes quickly. These oxides accumulate in the MME and adsorb preferentially on metallic surfaces such as the needle and the connection pin and can interfere with the quality of the voltammograms. To mitigate this, we recommend cleaning the needle daily by simply screwing it off, wiping it gently, and screwing it back in with the exact same tightness, and to clean the mercury weekly. Prior to mercury cleaning, we recommend to vigorously shake the MME to desorb mercury oxides. Then, instead of dismantling completely the MME, we suggest opening it only from the back, emptying the mercury, and collecting the clean mercury by pipetting from just below the surface oxidised layer before placing it back in the MME. Cleaning following the above procedure on a weekly basis was observed to be easier, faster, safer and overall, better for the capillary than less frequent cleaning leading to mercury oxide accumulation. This procedure was specifically developed for MetrohmTM MME; mercury

reservoirs from different manufacturers may not experience such rapid mercury oxidation. Health and safety instructions from manufacturers should be checked prior to manipulating the MME to limit mercury exposure and spillage (i.e., manipulating the MME above a tray and in a well-ventilated space with appropriate personal protective equipment, and with spill kit available nearby).

BioAnalytical Systems, Inc. (BASi)

The CLE-AdCSV method was further assessed on a BioAnalytical Systems, Inc. (BASi) electrochemical system at Oregon State University. This system was comprised of a Controlled Growth Mercury Electrode (CGME) cell stand connected to an Epsilon 92 electrochemical analyzer. The CGME was employed in Static Mercury Drop Electrode (SMDE) mode with a drop size of 14 and commercially available quadruple-distilled elemental mercury (Bethlehem Apparatus). The mercury reservoir of the CGME is enclosed under vacuum, and the dispensing of mercury drops from the reservoir of the CGME is accomplished with a solenoid valve. No compressed gas is required for this application, and the mercury does not readily oxidize in this setup; it does not require regular cleaning as for the Metrohm™ systems. The bevelled glass capillary (150 µm inner diameter; part # MF-2090), Ag/AgCl reference electrode (MR-2052), platinum wire auxiliary electrode (MW-1032), and Teflon-coated stir bar (ER-9132) were all included in the CGME Cell Stand Package purchased from BASi. The glass capillary and Teflon stir bar were wiped down with methanol prior to use, but otherwise were not cleaned before the cell conditioning process was begun. The voltametric cell used on this system is a Teflon (fluorinated ethylene propylene, FEP) cell originally manufactured by Princeton Applied Research (now Ametek), which had first been cleaned in concentrated Trace Metal Grade (TMG) aqua regia (TMG HCl and HNO₃; Fisher Chemical™) and stored in Milli-Q until conditioned for use.

Voltametric procedure

The procedure for the Metrohm™ application of the method is adjusted from Buck et al. (2007) and Abualhaija and van den Berg (2014) using the software NOVA 2.5 (Metrohm™). Three new drops were formed prior to the analysis by DP-AdCSV (Differential Pulse Adsorptive Cathodic Stripping

Voltammetry) using the following parameters: deposition at +0.05 V (optimisation presented hereafter) for 45 s to 3 min (depending on the sampling depth of the sample) while vibrating, 3 s of equilibration (no vibration), stripping from -0.25 to -0.6 V with a 6 mV step, 50 mV amplitude, 35 ms pulse time and 200 ms interval time. For the BASi application of the method, analyses were accomplished as described by Buck et al. (2007) by DP-AdCSV using the software EpsilonEC and the following parameters: deposition at +0.05 V while stirring, 15 s of equilibration (no stirring), stripping from 0 to -0.85 V with a 6 mV step, 50 mV amplitude, 35 ms pulse width and 200 ms pulse period.

Reagent preparation

For the application of the method on the MetrohmTM system, the preparation of the SA solution is adjusted from Abualhaija and van den Berg (2014). SA (SA: 98% Acros OrganicsTM) stock solution of 20 mL at 0.1 M was prepared in Milli-Q water (Millipore, 18.2 M Ω) only once and stored in the fridge in a Metal Free LabconTM tube at pH < 1 (acidified with TMG HCl, FisherScientificTM; Abualhaija and van den Berg, 2014). From this stock solution, 20 mL of 5 mM at pH 2 were prepared regularly (around once a month) 24 hrs prior to use to ensure stability and homogeneity. Gentle heating of the stock solution (between 30 and 35 °C) was necessary to prevent the presence of a liquid organic phase. We followed the preparation suggested in Abualhaija and van den Berg (2014) in this work, but stock solution of lower concentration should ease its manipulation by limiting the formation of the organic phase. A batch of 250 mL of a 1 M borate/ammonia buffer was prepared by diluting boric acid (analytical reagent grade, Fisher ScientificTM) in 0.4 M ammonia (NH₄OH; 29% LaporteTM). Borate/ammonia buffer is classically used at 10 mM to adjust the pH around pH 8.2 (NBS scale; Millero et al., 1993) because it does not complex Fe, as opposed to stronger organic buffers (e.g., Gupta et al., 2013). Fe standards at pH 2 (acidified with TMG HCl) were prepared from a Fe stock solution, 1000 ppm (17.9 mM; BDHTM). A 50 μ M Fe standard was used for cell and tube conditioning, prepared monthly. A 2 μ M Fe standard was used to prepare the titrations, prepared weekly.

For the application of the method on the BASi, the procedures of Buck et al. (2007) were followed. Briefly, a 5 mM solution of SA (98+%, TCI America™) was prepared in 200 mL high purity methanol (LC/MS Grade Optima, Fisher Chemical™) and stored in the refrigerator when not in use. When prepared in methanol, the SA solution is stable for many months and does not require any further cleaning (Buck et al., 2007). A 1.5 M borate/ammonium buffer solution was prepared by dissolving high purity boric acid (99+%, Thermo Scientific™) in 0.4 N ammonium hydroxide (Optima, Fisher Chemical™). The buffer required further cleaning, which was accomplished by using a peristaltic pump (Gilson) and size 13 tubing (ColeParmer) to pump the solution through two sequential Chelex (BioRad™) cleaning columns. Prior to use, the cleaning columns were prepared with the same pumping setup and flushed with approximately 200 mL Milli-Q, followed by similar volumes of 10% TMG HCl, 0.024 M TMG HCl, another 200 mL Milli-Q, and finally 100 mL of 0.4 N ammonia hydroxide to ensure the column was conditioned to the buffer matrix. The first 50 mL of buffer passed through the columns after these steps were discarded, and the remainder collected in narrow mouth Teflon (FEP, Nalgene) bottle for use. The buffer was stored in the clean hood at room temperature to minimize the risk of precipitation. A 50 µL addition of the buffer to 10 mL sample was used in speciation analyses, achieving pH 8.2 (NBS scale). Dissolved Fe standards were prepared by dilution of a 1000 ppm Fe standard (atomic absorption spectrometry grade, AA; Fisher Chemical™) in 0.024 M TMG HCl and stored at room temperature (Buck et al., 2007).

Sample preparation

FeL titrations were obtained using sequential equilibration, whereby Fe additions are equilibrated for at least 2 hrs, before SA is added at least 15 min before starting the analysis, as previously described by Rue and Bruland (1995) and Buck et al. (2007, 2015, 2018). Analysis reproducibility was evaluated in 19 samples analyzed in duplicate (with one in triplicate, 20 comparisons). Overnight equilibration (minimum of 8 hrs) using the same SA concentration added 10 min after Fe additions was also applied for comparison in 24 samples (including 4 of the samples for which duplicate analysis was performed, 28 comparisons). For both equilibration, seawater aliquots were spiked with 10 mM of borate buffer and 25 µM of SA. Specific set of tubes were prepared for each equilibration.

The sets were composed of 16 tubes with DFe additions ranging from 0 to 15 nM (Table 2). Prior to preparation, samples were left to thaw overnight in the dark at room temperature, then energetically swirled. If duplicates were analysed within a few days, they were kept in the fridge. If more time was needed before the second analysis, they were frozen back at -20 °C. The samples analysed to evaluate the reproducibility and the impact of the equilibration procedure in this study were collected in the Western Tropical South Pacific in 2019 during the cruise GPpr14 (TONGA cruise; Guieu and Bonnet, 2019). For complementary information regarding DFe and FeL in those samples, please refer to Tilliette et al. (2022) and Mahieu (2023), respectively. Conditioning waters used for the application with the MetrohmTM systems was a mixture of deep waters collected during the GA13 FRidge cruise in the mid-Atlantic in 2017 and kept in the dark at room temperature in a 50 L carboy made of polycarbonate (Nalgene), while for the application with the PA3i systems, the conditioning seawater was surface waters collected in the Gulf of Mexico in 2015 kept frozen in 500 mL bottles made of fluorinated high density polyethylene (FHPE; Nalgene).

Peak height extraction from voltametric measurements

The treatment applied for the data presented in this work consisted of the conversion of the initial voltammograms into derivative scans, prior to automated peak height determination, completed by manual peak determination when necessary. This treatment was performed using the freely available ECDSOFT software following a procedure detailed in SM1. The use of the derivative peak height instead of the direct peak height or peak area is favoured in case of curvature of the baseline under the peak (Salaün et al., 2007; Cobelo-García et al., 2014). For example, if the baseline is approximated by a third polynomial, the derivative will transform it to a linear baseline, avoiding manual and user dependent definition of the baseline (Omanović et al., 2010). However, it is crucial that the half-width of the second derivative peak is unchanged for the treated dataset (e.g., complexometric titration). In our case, the half-width of the FeSA peak on second and fourth derivative scans was not impacted by the addition of Fe, meaning that both can be used for quantification purposes.

Result and discussion

Recommended conditioning procedures

Conditioning of the PTFE voltametric cell

A systematic decrease of the FeSA peak is observed when the voltametric system is not sufficiently conditioned (Gerringa et al., 2021), and deliberate conditioning of the system with Fe has been noted across the applications of the FeSA method (Rue and Bruland, 1995; Buck et al., 2007, 2012; Bundy et al., 2014). Here, we also observed a strong decrease of the signal with time in the voltametric cell in the absence of conditioning (Figure 1b), consistent with adsorption of Fe on cell walls, stirring device, and electrodes. To prevent such adsorption, we developed a procedure to saturate the adsorption sites with a high amount of Fe that consistently led to reproducible peak heights across the titration range. Figure 1 presents the difference in stability of the signal in a voltametric cell with and without conditioning (Figure 1a and b, respectively). The optimal conditioning procedure for the Metrohm™ voltametric PTFE cell consisted of leaving overnight (≥ 3 h) a buffered seawater sample spiked with 300 nM of Fe in the cell placed on the system and containing the electrode and stirring device. The concentration of 300 nM showed better peak stability than overnight conditioning with 50 and 150 nM of Fe while the addition of 25 μ M of SA had no apparent effect (results not shown). The conditioning sample spiked with 300 nM of Fe showed only 7 nM of Fe left after overnight conditioning (Figure 1a). The carried over DFe was effectively removed by 3 Milli-Q rinse of cell and a sacrificial buffered seawater sample containing 25 μ M of SA. The stability of the signal over 5 scans at different Fe concentration attests to the absence of further Fe adsorption and desorption, confirming the stability and inertia of the conditioning (Figure 1a). For optimal preservation of the conditioning, we suggest keeping the cell with a similar matrix as the analysed samples, i.e., seawater if possible, though Milli-Q can be used if seawater is limited.

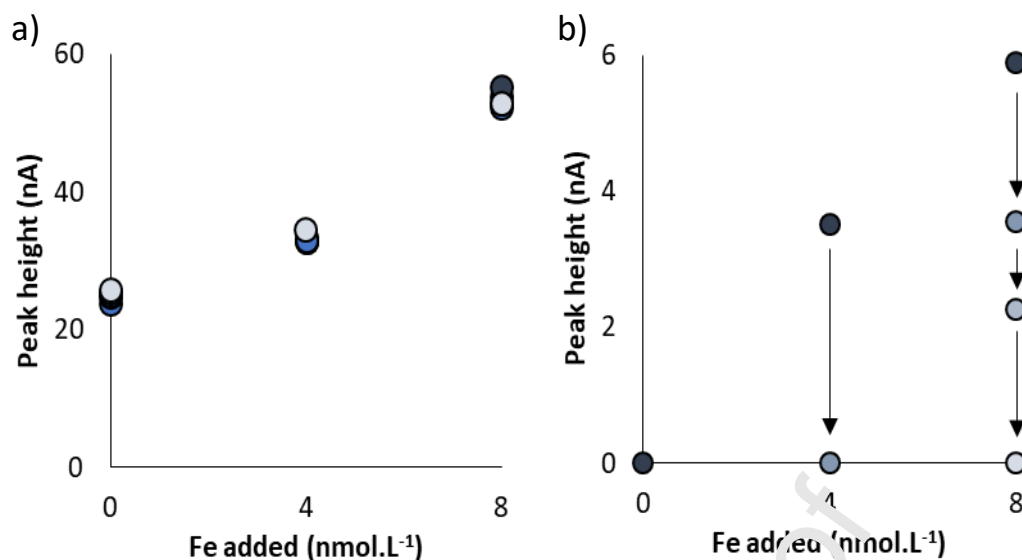


Figure 1. Stability of the FeSA₂ reduction signal in a buffered open-ocean seawater sample containing 25 μ M of SA on the Metrohm™ after a) overnight conditioning, initially spiked with 300 nM of and b) deconditioning of the cell by 15 min rinse with 0.5 M HCl and rinsed 5 times with Milli-Q. 5 scans were recorded if the peak was stable, or until the signal reached 0 nA if unstable. For each DFe addition, the first voltammogram recorded are darkest and become paler with time (90 s between voltammograms with 60 s deposition time).

Conditioning of polypropylene tubes

An empirical methodology was developed to condition the tubes used to prepare the titration aliquots of the samples (polypropylene Metal Free tubes, 50 mL, Labcon™). Prior to conditioning, the tubes are simply cleaned by an overnight acid bath at 1 M HCl and thorough Milli-Q rinse, since no difference was observed with tubes cleaned by successive week-long baths in Dekon detergent, 1 M HCl and 0.1 M HCl (results not shown). In absence of tube conditioning, the titrations were not showing the peak corresponding to the FeSA₂ complex, even at high DFe. The preparation of several sacrificial titrations at regular DFe addition was not solving the issue.

The most efficient conditioning procedure consisted of a weeklong conditioning with high Fe concentrations (minimum of 50 nM; Table 2) added to buffered seawater containing 25 μ M of SA, and swirling several times a day every day. At the end of the week of conditioning, the tubes were emptied, rinsed twice with Milli-Q, and filled with a titration. If the titration analysis showed a linear response at high additions giving the same slope as a post-titration spike (i.e., not equilibrated with SA in the tubes but added directly to the cell; Whitby et al., 2018), then the tubes were considered sufficiently conditioned for analytical work. In the absence of swirling during the weeklong

conditioning, the tubes required the preparation of 5 to 10 titrations before sufficient conditioning was achieved. Between titrations, the tubes were filled with 20 mL of Milli-Q and energetically shaken for rinsing, and kept dry when not in use. Following previous recommendation (e.g., Abualhaija and van den Berg, 2014; Gerringa et al., 2014), we recommend using, when possible, bulk open ocean seawater available at a sufficient volume both to (1) condition all sets of tubes and the cell, and (2) be used as a reference seawater. A set of experiments exploring the flexibility of the conditioning procedure were performed and are presented in SM4.

Table 2. DFe additions added to buffer seawater for conditioning of 50 mL polypropylene MetalFree tubes (Labcon™) and PFA vials (Saville™). For the polypropylene tubes, 25 μ M SA is also added with the Fe for conditioning, and the tubes are regularly swirled to speed up conditioning. For the PFA vials, SA is added at the end of each round of conditioning. See manuscript for detailed outline of the conditioning procedures.

polypropylene tubes	DFe for sample titrations	0	0	0.8	1.6	2.5	3	3.5	4	4.5	5	6	7	8	10	12	15
	DFe for conditioning	50	50	50	50	50	50	50	50	50	50	50	70	80	100	120	150
PFA vials	DFe for sample titrations	0	0	0.10	0.25	0.50	0.75	1	2	2.5	3	4	5	7.5	10		
	DFe for conditioning	10	10	10	10	10	10	15	20	25	30	40	50	100	150		

Conditioning of PFA vials

A similar procedure using high Fe concentrations is sufficient for the conditioning of the 15 mL flat-bottom PFA vials (Saville™) commonly used for Fe speciation titrations with SA. New vials are typically cleaned first in a soap bath (0.8% Citrad™ in distilled water) and then acid-cleaned only once by soaking in concentrated aqua-regia (TMG HCl and HNO₃; Fisher Chemical™) for a week. It is possible that this aqua regia step is not necessary, and could be replaced with a longer (e.g., month-long) soak in a weaker acid bath (e.g., 10% TMG HCl), but we have not tested this. Following the aqua regia bath, the vials are stored in Milli-Q for at least one more week, after which the conditioning procedure can begin. New vials, or vials newly applied to Fe speciation measurements with SA, are conditioned with mock titrations containing seawater, buffer, and high Fe additions (Table 2). A minimum of 10 nM Fe is added to the vials that will be used for the lowest (<1 nM) sample titration additions, 10-fold Fe additions are used thereafter, and 15-fold higher for the two

highest planned additions (Table 2). The additions are left in the buffered seawater samples for several days in the first round (e.g., over the weekend), and three iterations with the additions left overnight. For these overnight soaks, 25 μM SA is added to the vials the following morning, allowed to equilibrate at least 15 minutes, and the contents analyzed; the content of the last titration vial, with the highest added Fe concentration, is left in the cell overnight to condition it and analyzed again in the morning to assess consistency. Once reproducible peak heights are observed in these conditioning titrations, the vials are filled with a mock sample titration and analyzed for verification. Following analysis of the last addition in the mock sample titration, 5 nM of Fe is added directly to the voltametric cell as a post-titration spike to verify (1) that the peak heights at the end of the titration sample had increased in proportion to the Fe additions and (2) the absence of Fe loss during the equilibration (e.g., Whitby et al., 2018). If the response is linear, the vials and voltametric cell are sufficiently conditioned for sample analyses. The post-titration spike continues to be employed throughout sample analyses as a tool not only for verifying conditioning but also for ensuring that the natural ligands in the samples have indeed been titrated.

Conclusion on the conditioning procedure

Optimum conditioning procedures vary depending on different voltametric systems, tubes, and vials. In all cases, saturation of the adsorption sites seems to occur through the formation of various Fe species that are no longer labile to SA at 25 μM . Once the material is conditioned, it can be safely used if regular duplicate or reference water analysis are consistent. In term of conditioning process, we hypothesise that for weeklong conditionings, SA could help for optimal distribution of Fe at the surface of the vessels over the weeklong conditioning necessary for stability of the slowly formed Fe 'layer' or 'coating'. The FeSA_2 would slowly dissociate near the tube wall, scavenging Fe from the solution. Regular swirling would optimize the conditioning by ensuring optimal flux of Fe to the tube wall. It is not surprising that the amount of Fe and time requirement differ between the voltametric system and the tubes, since differences in Fe adsorption behaviour with materials has been established in previous work (Fischer et al., 2007). The stability of the signal shown in Figure 1a, 2 and 3, however, attests to the non-lability of Fe after application of the procedures developed for our

equipment. We know from practical experience that conditioning can be achieved with lower Fe additions, with Fe added with and without SA, and without swirling the tubes or vials; however, what we outline here and in Table 2 represents the fastest way we could achieve after months of experimenting.

Effect of the deposition potential

The impact of the deposition potential on the FeSA reduction peak current was investigated in the conditioning seawater for the Metrohm™ application, buffered and spiked with 25 μM of SA (Figure 2). The experiment was performed twice starting at -0.10 V up to +0.05 V, and twice starting at +0.06 V down to -0.10 V. Increments were of 0.02 V. By applying a deposition potential of +0.05 V, the sensitivity of the method is increased by around 3-fold and 1.8-fold compared to the previously applied values of -0.05 V (Rue and Bruland, 1995) and 0 V (Buck et al., 2007; Abualhaija and van den Berg, 2014), respectively. A deposition potential above 0 V was previously attempted (Buck et al., 2007) and produced a similar peak height at +0.05 V relative to 0 V and then a steep decrease of the signal at +0.1 V. In our case, the signal is higher at +0.05 V relative to 0 V. The contrasted results obtained by the different analysts suggest that the influence of the deposition potential is sample dependent.

The sensitivity of the SA method also decreases with sample depth in the Pacific relative to the Atlantic (Rue and Bruland, 1995; Buck et al., 2007, 2015, 2018), which was hypothesized to result from distinctions in the composition and/or structure of the DOM with the aging of water masses (Buck et al., 2018). The sensitivity loss is generally compensated by the deposition time used, ranging from 90 s to 600 s in surface and deep Pacific Ocean samples, respectively (Buck et al., 2018). Using a higher deposition potential of +0.05 V, the deposition time required in our study ranged from 45 s in surface samples to 150 s in deep samples collected in the Western Tropical South Pacific. It is well known that the adsorption of organic compounds can lower the sensitivity of the AdCSV method of Fe detection (e.g. Yokoi and van den Berg, 1992). Our results suggest that a higher deposition potential limits the adsorption of negatively charged refractory DOM at the mercury electrode in

Western Tropical South Pacific waters. Deposition potentials higher than +0.07 V were not tested to limit oxidation of the mercury electrode and a deposition potential of +0.05 V was chosen as the optimal value. This deposition potential allowed analysis of a complete titration of 16 aliquots with triplicate voltammograms in less than 1 hour, even for deep samples, a significant improvement compared to other studies (e.g., Buck et al., 2007, 2018; Cabanes et al., 2020). The deposition potential value of +0.05 V could be of specific interest in samples containing high concentrations of DOM such as coastal samples.

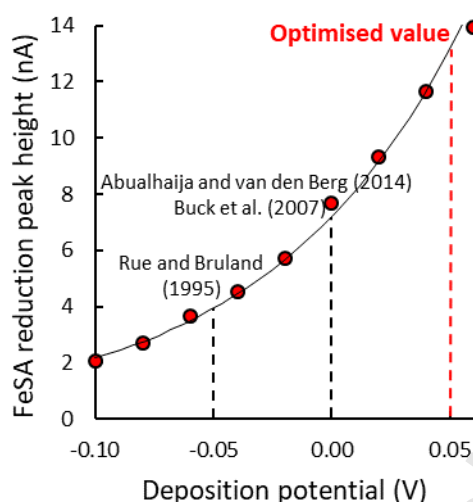


Figure 2. Reduction current of the FeSA peak after 45 s deposition as a function of the deposition potential applied in a seawater sample buffered to pH 8.2 containing 25 μ M of SA. Previously published values (-0.05 V and 0.00 V) and the one selected in this study (0.05 V) are noted. An exponential fitting is shown for visual

These findings also suggest that the deposition potential for this method may provide useful insights into the composition and/or electroactivity of the DOM in natural samples. The relation between the trace metal binding strength by DOM and the deposition potential applied in anodic stripping voltammetry (ASV) has been used in the past, notably for copper, and is referred to as pseudopolarography (e.g., Garnier et al., 2004; Louis et al., 2008, 2009). The relation between the peak intensity and the deposition potential presented here and in previous work could be representative of the competitive adsorption on the mercury drop between the electroactive DOM and FeSA₂ (Rue and Bruland, 1995; Buck et al., 2007; Abualhaija and van den Berg, 2014; this study).

This was not explored in our work, but we highlight that the dependency of the signal intensity to the deposition potential in AdCSV in presence of SA may provide additional information to characterise electroactive DOM.

Validation of ligand titrations

For the MetrohmTM systems, the titration presented in Figure 3 illustrates two features classically observed: Fe carry-over from previous analysis with the first aliquot, and saturation of the mercury drop electrode at high Fe concentration. For the BASi systems, two different analyses are presented in Figure 4: one of the seawater used for conditioning the tubes, and one of the same seawater spiked with 2 nM of deferoxamine B (DFO-B; Figure 4b). The addition of DFO-B, a siderophore of high affinity with Fe, is an easy and reliable way to validate the CLE-AdCSV application, previously performed in a similar application in the absence of natural ligands (e.g., Rue and Bruland, 1995; Abualhaija and van den Berg, 2014). Here, we performed the DFO-B addition in the presence of the natural ligands to verify the absence of interfering interaction between the natural ligands and the detection of FeSA₂ at the mercury drop electrode, a process reported in previous work for other added ligands with humic substances (Laglera et al., 2011). Our results show the expected increase in L_{Fe} corresponding to the 2 nM DFO-B added (with regards to the uncertainty of the analyses), and an increase in $\log K_{Fe/L}^{cond}$, in line with the high affinity of DFO-B for Fe. The lower $\log K_{Fe/L}^{cond}$ found here compared to previous characterization of DFO-B at similar SA concentration ($\log K_{Fe/L}^{cond} > 14$; Rue and Bruland, 1995; Bundy et al., 2018) illustrates a fundamental characteristic of the $\log K_{Fe/L}^{cond}$ determination by CLE-AdCSV, being an averaged value of the individual $\log K_{Fe/L}^{cond}$ of all the binding sites in competition against the added ligand (here, the natural ligands and the added DFO-B).

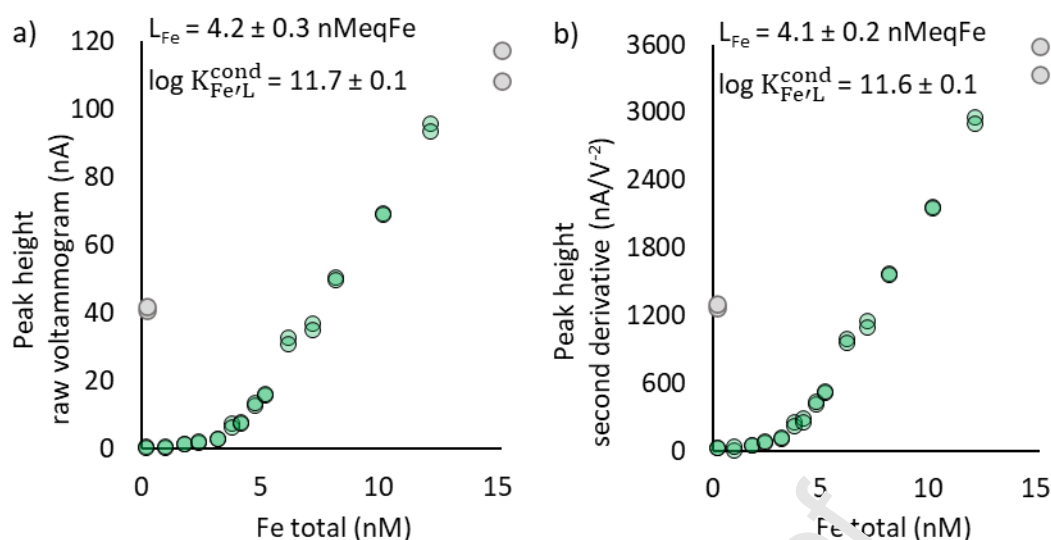


Figure 3. a) Peak height and b) second derivative of the titration of the FRic ze seawater used for voltammetric cell and tubes conditioning with 25 μM of SA and buffered at 8.18 with 10 mM of borate acquired with the MetrohmTM system. Duplicates voltammograms were recorded with a deposition time and potential of 60 s and +0.05 V, respectively. The sample was equilibrated following the sequential procedure equilibration. The green dots represent the data selected to determine L_{Fe} and $\log K_{\text{Fe/L}}^{\text{cond}}$ (procedure detailed hereafter). Grey dots represent the discarded data, corresponding to carry-over Fe in the cell from previous analysis at the start of the titration, and saturation of the working electrode with the last aliquot.

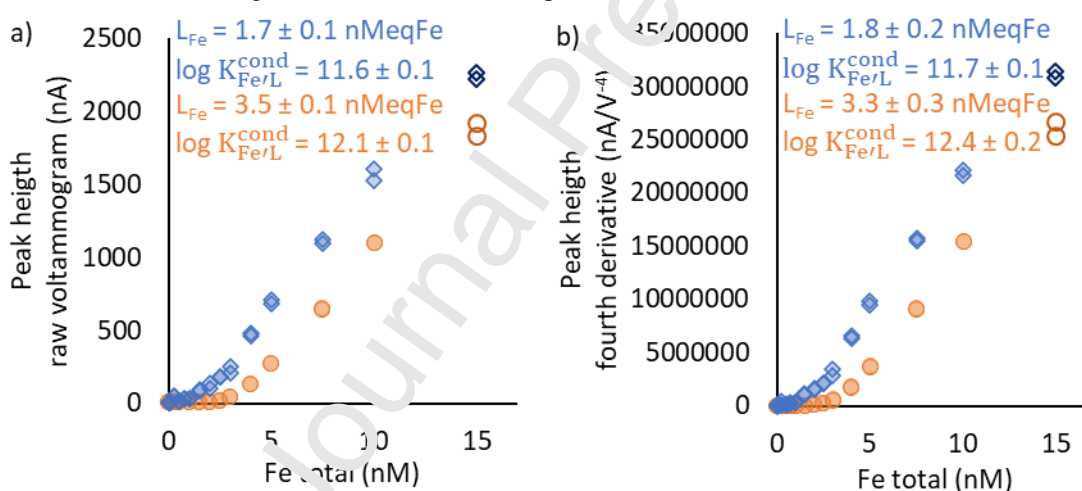


Figure 4. a) Peak height and b) fourth derivative of the titration of the Gulf of Mexico seawater used for tubes conditioning with 25 μM of SA and buffered at 8.18 with 10 mM of borate without (blue diamonds) and with (orange circles) addition of 2 nM DFO-B acquired with the BASi systems. Duplicates voltammograms were recorded with a deposition time and potential of 90 s and +0.05 V, respectively. The sample was equilibrated following the sequential procedure equilibration. The last points of the titrations (empty symbols) correspond to the 5 nM Fe spike performed in the last aliquot.

We compare in Figure 2 and 3 the results obtained with manual determination of the peak height and with the automated approach developed to ease and fasten data handling. For both applications (i.e., with the MetrohmTM and the BASi, Figure 3 and 4, respectively), the fast automated approach resulted in similar Fe-binding ligand characteristics that the time-consuming manual determination. Several

adjustments were necessary to ensure optimal efficiency of the software ECDSOFT and avoid manual treatment of some voltammograms. For the voltammograms acquired with the Metrohm™ systems, the optimal treatment consisted of using the second derivative scans and increasing the number of data points composing the voltammograms by a factor 3, and with the BASi, the optimal treatment was using the fourth derivative without increasing the number of data points. The variations of the automated peak determinations are attributed to differences in the voltammogram acquired with the two set up compared here, notably in terms of peak height range. Future users should compare the different parameters available within ECDSOFT to define the optimal automation of the peak determination corresponding to their application.

For the application with the Metrohm™ systems, the conditioning seawater was kept in the dark at room temperature in a 50 L carboy (polycarbonate, Nalgene), while for the application with the BASi systems, the conditioning seawater was kept frozen in several 500 mL bottles (FHPE, Nalgene). Repeated titrations of the conditioning seawater kept in the carboy showed a drift in L_{Fe} toward higher values with time and emptiness of the carboy (results not shown), suggesting an impact of the aging of the DOM and/or stratification in the carboy. We suggest not to sample and store reference seawater in large polycarbonate carboy, but such water can be used for conditioning.

A post-titration Fe spike of 5 nM was performed in the final aliquot being analyzed to confirm the saturation of the organic ligands (Figure 3). For the titration in the presence of DFO-B, the spike confirms the saturation of the natural ligands, and the absence of saturation of the mercury drop. For the titration in absence of DFO-B, the spike confirms the saturation of the natural ligand, but also the saturation of the mercury drop electrode for the final aliquots. The aliquots for which the linearity is impacted by the saturation must be discarded for the interpretation. Guidance for the data selection and interpretation of ligand titrations are provided in the following section.

Recommendations for the interpretation of ligand titrations

The development of ProMCC software has substantially eased the interpretation of ligand titrations (Omanović et al., 2015), although the results remain notably dependent on the choice of the

mathematical treatment used to retrieve the $\log K_{\text{Fe/L}}^{\text{cond}}$ of the natural ligand, on the definition of the sensitivity of the method (e.g. Omanović et al., 2015) and on the data selection made by the analyst (Buck et al., 2012). It is sometimes necessary to remove outliers but currently, the definition of outlier is subjective. We propose here a procedure to treat titration data in a systematic way to statistically exclude potential outliers independently, and to simultaneously model ligand characteristics using the most common fitting procedures (Ružić, 1982; van den Berg, 1982; Scatchard, 1949; Gerringa et al., 2014). All the results presented hereafter were collected using the Metrohm™ systems.

Definition of the sensitivity

The first step was to assess how to best define the sensitivity (S) of the measurement. The definition of S should be tested for every application of a CLE-AdCSV method on a set of natural samples. The simplest and most straightforward approach for this is the post-titration spike as a verification of the linearity of the final internal titration points. We also compared the results obtained by using S determined from the three last linear aliquots with the mathematical fit option given in ProMCC. Replicate titrations were fitted using both methods, the differences between duplicates in L_{Fe} (ΔL_{Fe}) and between $\log K_{\text{Fe/L}}^{\text{cond}}$ ($\Delta \log K_{\text{Fe/L}}^{\text{cond}}$) were determined, and the standard deviations of the ΔL_{Fe} and $\Delta \log K_{\text{Fe/L}}^{\text{cond}}$ obtained with each method compared. For L_{Fe} and S , the standard deviation was divided by the mean value for all the duplicate titrations mentioned in Table 3, while for $\log K_{\text{Fe/L}}^{\text{cond}}$, the standard deviation was divided by the acknowledged range of values covered by a single detection window (i.e., 2; Apte et al., 1988; Gerringa et al., 2014). Here, the most consistent results were obtained when S is defined with the 3 last aliquots of the titration, with 22% of residual standard deviation (RSD) for ΔL_{Fe} , against 46% for the mathematical fitting. Differences between the two fittings for $\Delta \log K_{\text{Fe/L}}^{\text{cond}}$ were negligible in comparison to the differences in ΔL_{Fe} . The definition of S with the 3 last aliquots has thus been implemented in our procedure. Despite recommendations from Gerringa et al. (2014) to use 4 aliquots, our results showed that in our case the accuracy was not impacted by the use of 3 or 4 aliquots (results not shown). This could be attributed to the range of concentration of D_{Fe} considered in our titrations, up to 15 nM, compared to up to 10 nM used by

Gerringa et al. (2014). This emphasizes the importance of extending the titration well into the linear portion to ensure optimal definition of the sensitivity.

In our case, the relative standard deviation (RSD) of ΔL_{Fe} and $\Delta \log K_{Fe/L}^{cond}$ was independent of the high RSD (e.g., poor reproducibility) in S values between duplicate analysis. We attribute the high S RSD to the presence of mercury oxides in the MME in the case of the MetrohmTM system. Indeed, despite daily cleaning of the needle ensuring good quality of the scan and accurate determination of L_{Fe} and $\log K_{Fe/L}^{cond}$, mercury oxides were accumulating in the mercury reservoir over the week. We suggest that the daily cleaning of the needle is not enough for optimal reproducibility of the S of the MetrohmTM system, and that the formation and/or impact of the mercury oxides are variable from one week to another. Even if it does not impact the ΔL_{Fe} and $\Delta \log K_{Fe/L}^{cond}$ obtained, the fluctuation of the S is to be kept in mind when using and comparing results obtained on MetrohmTM systems.

Table 3. Deviation between duplicate analyses on L_{Fe} , $\log K_{Fe/L}^{cond}$ and S with two definitions of S. The relative standard deviation (RSD) corresponds to the standard deviation divided by the mean for ΔL_{Fe} (5.1 nMeqFe) and ΔS , and by the acknowledged range covered by a single detection window for $\Delta \log K_{Fe/L}^{cond}$ (2; Apte et al., 1988; Gerringa et al., 2014).

Definition of the sensitivity:	Using the 3 last aliquots			Fitted by ProMCC		
	ΔL_{Fe} (nMeqFe)	$\Delta \log K_{Fe/L}^{cond}$	ΔS ((nA/V ²)/s)	ΔL_{Fe} (nMeqFe)	$\Delta \log K_{Fe/L}^{cond}$	ΔS ((nA/V ²)/s)
ST6-21	0.0	0.3	-0.8	-0.7	0.1	-3.2
ST6-20	3.0	-0.5	-3.9	8.1	-0.3	1.7
ST6-11	0.5	0.0	-8.1	0.6	0.0	-8.2
ST6-7	-0.6	-0.5	-4.1	3.6	-0.6	-3.9
ST6-5	0.5	-0.3	1.5	2.4	-0.3	5.7
ST6-3	-1.7	0.0	-4.7	-2.2	-0.1	-7.0
ST2-7	0.0	-0.2	-0.4	3.2	-0.3	0.3
ST7-17	0.0	0.1	-3.2	0.7	0.0	3.2
ST7-17_2	-0.8	-0.1	-3.2	-1.5	0.0	-3.9
Standard deviation	1.3	0.3	2.8	3.2	0.2	4.3
Relative standard deviation	22%	14%	69%	46%	11%	82%

The options offered by the software ProMCC of linear or logarithmic fitting of the sensitivity did not limit the dispersion of the calculated L_{Fe} (results not shown). Although the mathematical approach of sensitivity fitting is the (only) theoretically correct approach, and as such, would be expected to

provide better results, it is more impacted by signal variability, because it uses all titration points for the calculation of S and not only the final 3 additions. The reduction current at low DFe additions is relatively more variable (less accurate) than at higher DFe additions, and thus the mathematical fitting might provide a less robust sensitivity than the final 3-point approach. The use of the “final 3-addition” approach is justified by the obtained better reproducibility with our dataset, as shown above. However, we still recommend comparing different approaches in sensitivity determination to justify the choice made and in particular, to verify the linearity of the final titration points with a post-titration spike.

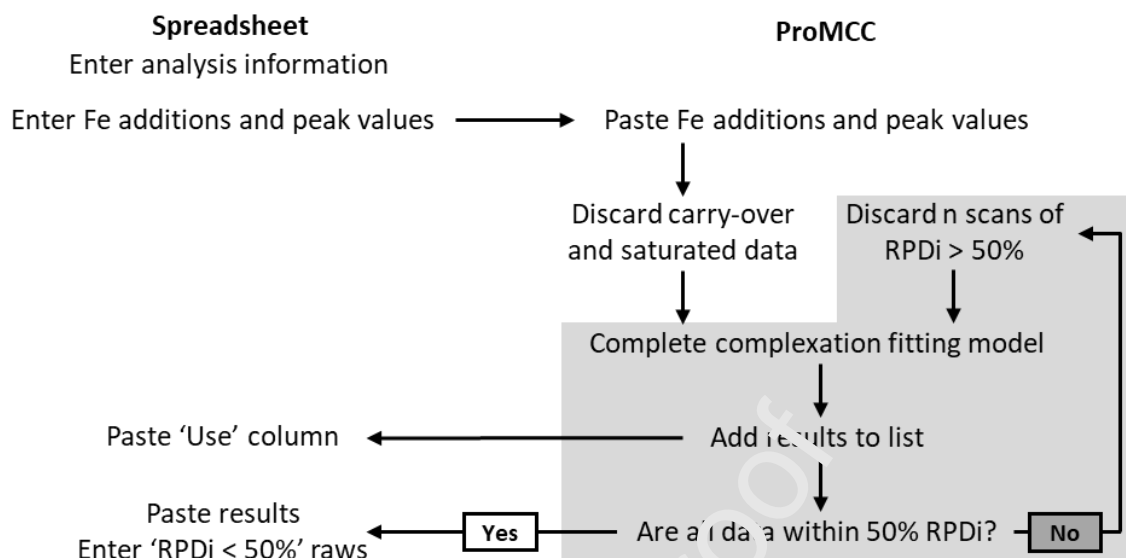
Step-by-step interpretation of the titration

The procedure developed for the interpretation of ligand titration data relies on the combined use of ProMCC and of a spreadsheet specifically prepared to keep track of the successive fittings and define the quality flag of the titration (Figure 5; SM2; SM3). A step-by-step description of the procedure is detailed in SM2 and included within the spreadsheet (SM3). The procedure we propose here allows a more reliable selection of the data points retained for the fitting by statistically identifying voltammograms of poor quality that can bias the calculated FeL characteristics.

Briefly, the user first needs to enter analysis information as requested in the spreadsheet and add the titration data to both the spreadsheet and ProMCC. From ProMCC, a pre-selection is made, based on the visual presence of carry-over Fe (high values for the first aliquot) or saturation of the titration at high added Fe concentration (flattening of the curve; Figure 2). A first “Complete Complexation Fitting Model” is then performed, “Add Results to list...” clicked, and the “Used” column of the “Data” tab copied in the spreadsheet. The graphical error of the titration presented as Relative Percentage Difference (RPDi) calculated in ProMCC is then used. RPDi corresponds to the dispersion of each data point from the fitted curve obtained by the “Complete Complexation Fitting Model”. Data points with an RPDi higher than 50% are discarded, in order of decreasing RPDi values. The RPDi values for all data from all aliquots are considered because this step aims to discard voltammograms of poor quality, not to evaluate the validity of an aliquot. If all the voltammograms recorded for an aliquot have an issue (e.g., due to contamination or problem during the preparation),

they will end up being discarded within the process. Following each data removal step, the “Complete Complexation Fitting Model” fit is performed, “Add Results to list...” clicked, and the “Used” column copied in the spreadsheet. The identification of lower quality datapoints and fitting steps are reproduced until all data show an $RPDi < 50\%$. The $RPDi$ used to define the validity of the data is automatically calculated in ProMCC, and, therefore, the data selection is not impacted by the analyst, who keeps a detailed record of the successive treatment with the spreadsheet. The $RPDi$ threshold value, however, could be adjusted for different applications and become a coefficient traducing the overall quality of the titrations for datasets.

a) Complexometric titration fitting



b) Definition of the quality flag

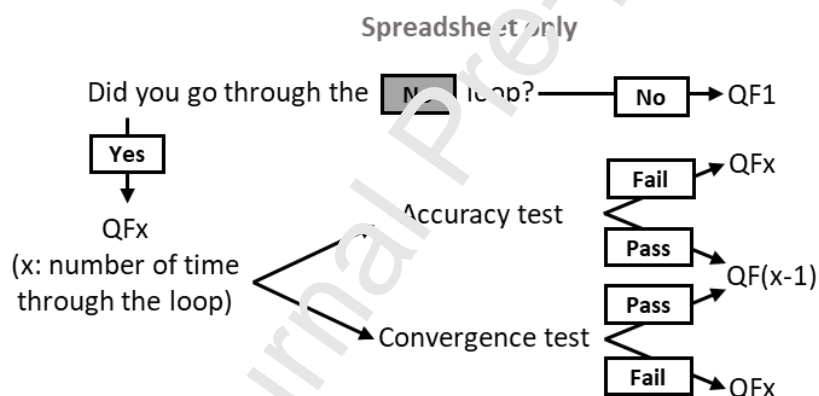


Figure 5. Diagram describing a) the procedure developed for the interpretation of ligand titration data, with n corresponding to the number of voltammograms recorded for each aliquot and RPD_i is the Relative Percentage Difference, and b) the procedure defining the quality flag (QF) of the titration. The QF is lowered by one even if only one of the tests (convergence or accuracy) is successful.

Automated determination of the quality flag within the spreadsheet

A quality flag (QF) system was implemented to rapidly visualise the confidence in the results with values ranging from 1 to 4, 1 being highly confident. Assignment of a QF to titration results as a whole allows for a rapid comparison of data quality in database archives of speciation measurements. Additionally, to our knowledge, there are no open access tools for users to keep track of the choices made when fitting titration data (e.g., number of replicates of each titration point, how outliers were defined and how many (if any) were discarded, which ones, how the sensitivity was defined, etc.).

This motivated the development of a spreadsheet combining the record of the metadata of the analysis, the record of the titration data, and the visualisation of the whole and selected complexometric data. The spreadsheet is intended to be used in tandem with ProMCC. This spreadsheet (SM3) is perfectible and is open to user's suggestions.

The QF value is based on three aspects (Figure 5b). The first relates to the number of fittings performed during the data selection procedure to reach a $RPDi < 50\%$ for all data points, with the QF being equal to the number of fittings having been performed. The second, which is automated, relies on the errors on L_{Fe} and $\log K_{Fe/L}^{cond}$, and the averaged error given by ProMCC. For L_{Fe} , an error of $\pm 10\%$ of the RSD or less was accepted (in our case, ± 0.5 nMeqFe). For $\log K_{Fe/L}^{cond}$, an error of ± 0.2 is accepted, corresponding to $\pm 10\%$ of the range of 2 unit of $\log K_{Fe/L}^{cond}$ covered by an analytical window (Apte et al., 1988; Gerringa et al., 2014). Accordingly, the limit of the criteria on the average error calculated by ProMCC as root-mean-square error (RMSE) is 20%. If two of the tests performed on L_{Fe} , $\log K_{Fe/L}^{cond}$ and average error are successful, the QF value previously defined by the number of fittings and data selection performed to reach $RPDi < 50\%$ is lowered by one (meaning the confidence is increased).

The third aspect defining the QF relies on the convergence of the fittings. Successive fittings can lower the error on the parameters, but the parameter can show similar results in terms of L_{Fe} and $\log K_{Fe/L}^{cond}$ despite data points having been discarded, meaning that the initial fitting was accurate. We implemented an automated verification of the convergence of L_{Fe} and $\log K_{Fe/L}^{cond}$ along successive fittings and data selection. The QF is lowered by one if the values change by less than 20% of the method accuracy, so in our case by 0.1 nMeqFe for L_{Fe} and by 0.04 for $\log K_{Fe/L}^{cond}$. The rules to define the QF based on the error and on the convergence of the fittings are not cumulative, meaning that the QF cannot be lowered by more than one level.

In summary, the QF determination for the procedure developed for a single ligand class will flag the results of a titration from 1-4, with 1 being highest confidence, and we recommend that titrations that

receive a QF flag of 3 and 4 to be carefully compared to the rest of the dataset to decide whether to integrate the results into the final dataset.

Reproducibility of ligand titrations

The reproducibility of ligand titration and data treatment procedure was compared on 19 samples run in duplicate (including a triplicate, 20 comparisons). Results of the treatment of these analyses are presented in Figure 6 and the data table is presented in SM4. The samples were randomly chosen within a set collected in the Western South Tropical Pacific in 2019 (Guieu and Bonnet, 2019) covering a large range of biogeochemical conditions (e.g., DFe from 0.13 nM to 1.09 nM; Tilliette et al., 2022), with the area being impacted by intense diazotrophic and hydrothermal activity.

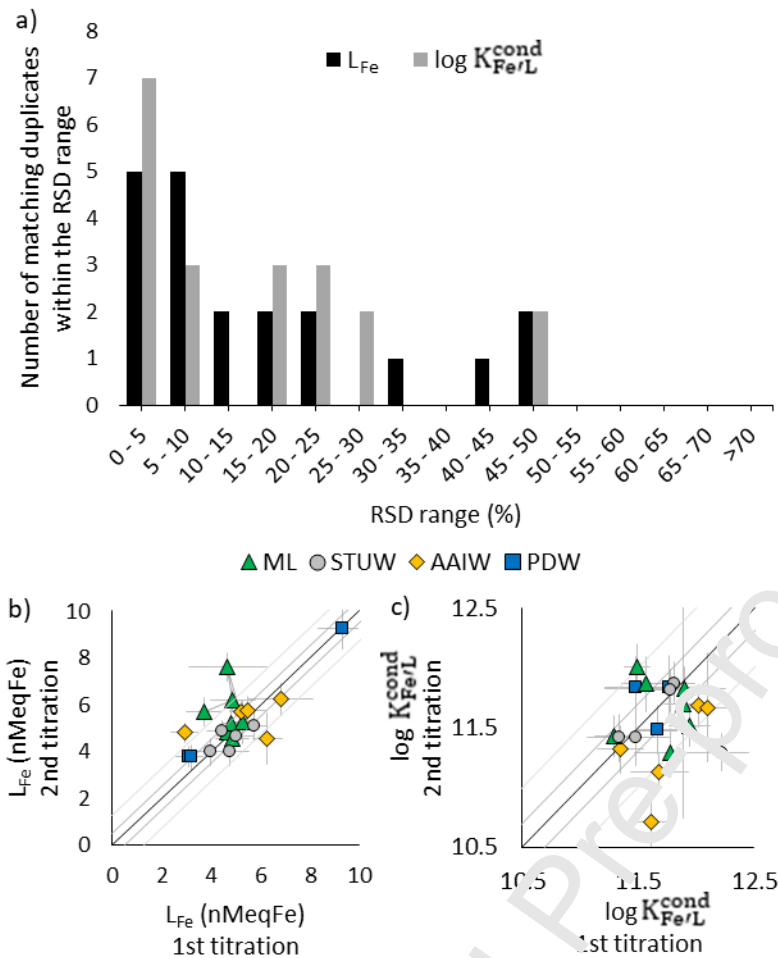


Figure 6. a) Distribution of the RSD of the L_{Fe} and $\log K_{Fe/L}^{cond}$ values and 1:1 plots for b) L_{Fe} and c) $\log K_{Fe/L}^{cond}$ of duplicate titration performed with the sequential equilibration. For the 1:1 plots, the results are shown in function of the water masses, namely the Mixed Layer (ML; green triangles), the Subtropical Underwater (STUW; grey circles), the Antarctic Intermediate Water (AAIW; yellow diamonds), and the Pacific Deep Water (PDW; blue squares). The grey lines correspond to 10 and 25% RSD of the main value for all titrations for L_{Fe} (5.1 nMeqFe) and of the range covered by the detection window for $\log K_{Fe/L}^{cond}$ (2).

The RSD between duplicates was calculated relative to the average value obtained between duplicates for L_{Fe} and relative to the range of $\log K_{Fe/L}^{cond}$ covered by a single detection window (2; Apte et al., 1988; Gerringa et al., 2014). Here, 50% of the duplicates agreed within 10% of the RSD for L_{Fe} and $\log K_{Fe/L}^{cond}$, and up to 80% within 25% of the RSD (Figure 6a). Meanwhile, the diazotrophic and hydrothermal processes of the area were responsible for L_{Fe} and excess L_{Fe} ($eL_{Fe} = L_{Fe} - DFe$) mean values of 5.1 ± 1.4 and 4.8 ± 1.3 nMeqFe, respectively. This is much higher than typically observed in open ocean samples. For comparison, a mean eL_{Fe} of 1.9 ± 1.1 nMeqFe was reported in the eastern tropical South Pacific, east of our sampling location (Buck et al., 2018). The agreement between

duplicate analyses is, therefore, rather high, with regard to the intense biogeochemical processes at play and of their impact on the Fe-binding properties of the DOM.

Interestingly, a relationship between the $\log K_{\text{Fe/L}}^{\text{cond}}$ and the time separating the duplicate analyses emerged for the samples collected in the Antarctic Intermediate Waters (AAIW; Figure 6c). The majority of the duplicates performed in other water masses did not show a similar offset in the second analysis. This offset could suggest a specific aging behaviour of the ligand assemblage in these samples, but the influence of mercury oxidation and re-freezing of the sample are not excluded. The change in $\log K_{\text{Fe/L}}^{\text{cond}}$ was not coupled to a change in L_{Fe} , suggesting a decoupling between the amount and the strength of the Fe-binding sites of the DOM. While other studies concluded on the limited impact of the aging of the DOM following similar freezing and thawing treatment (Fourrier et al., 2022; Fonvielle et al., 2023), our results suggest a potential impact on the Fe-binding sites of the DOM found in the AAIW.

Comparison of equilibration procedure on speciation parameters

It has been suggested that a shorter equilibration times could overestimate L_{Fe} and $\log K_{\text{Fe/L}}^{\text{cond}}$, as some dissociation kinetic of Fe and natural ligands could be too slow in absence of adjunctive mechanism between natural and added ligands (Gerringa et al., 2014; Laglera and Filella, 2015; Gerringa et al., 2021). However, to date, the impact of the equilibration time on the results obtained using SA have not been documented. Here, we compared the sequential and the overnight equilibration procedures on 24 samples collected in the Western South Tropical Pacific (Guieu and Bonnet, 2019), including 4 samples run in duplicate with sequential equilibration (28 comparisons). The results are shown in Figure 7, and the data table is presented in SM4. Half of the duplicates were performed within two days between first and second analyses, and the other half within one month. There were no trends emerging in relation to the storage time.

The deposition time requirement was on average 1.6-fold lower with the sequential equilibration than with the overnight equilibration, and a higher deposition time was required for deep samples (SM4), in line with previous studies (e.g., Buck et al., 2018). The lower deposition time requirement in our

application (from 45 s in surface samples to 150 s in deep samples; SM4) compared to previous study (60 s to 600 s; Buck et al., 2018) is explained by our optimised deposition potential of +0.05 V and by the technical specificity of the system used, such as the size of the mercury drop and stirring efficiency. The lower sensitivity observed for overnight equilibration has been previously attributed to the slow formation kinetics of the electro-inactive FeSA_2 complex (Abualhaija and van den Berg, 2014), but this was not experimentally proven. Such phenomenon could be an issue because the calibration of the added ligand depends on the specific stoichiometry of the complexes formed, which need to be well known and stable in time. However, for SA, the β_{FeSA} calibrated by Abualhaija and van den Berg (2014) by overnight equilibration and the β_{FeSA_2} calibrated by Buck et al. (2007) with sequential equilibration result in α_{FeSA} of 123 and in α_{FeSA_2} of 79 for 25 μM of SA, respectively. This leads to a shift of 0.2 in $\log K_{\text{Fe/L}}^{\text{cond}}$, lower than the error between most of the duplicates shown in the previous section. This suggests a limited impact of the calibration choice in our application. Also, other results (not shown) obtained while conditioning tubes of higher surface contact with the sample (15 mL, MetalFree LabconTM) suggest that instead of a slow change in SA speciation, a weak interaction with the tube walls could explain the decrease of the signal with the equilibration time. This hypothesis is, however, still under investigation and is not yet confirmed. Another possibility could be the slow dissociation of FeSA_2 toward inorganic forms of Fe such as colloids and/or Fe oxyhydroxides. Indeed, it was recently shown that the solubilization of Fe oxyhydroxides by humic substances decreased with the age and stability of Fe oxyhydroxides (Dulaquais et al., 2023). A similar phenomenon could happen during the equilibration with SA, as Fe oxyhydroxide stabilization could pull the equilibrium toward their formation and, concomitantly, toward FeSA_2 dissociation with time.

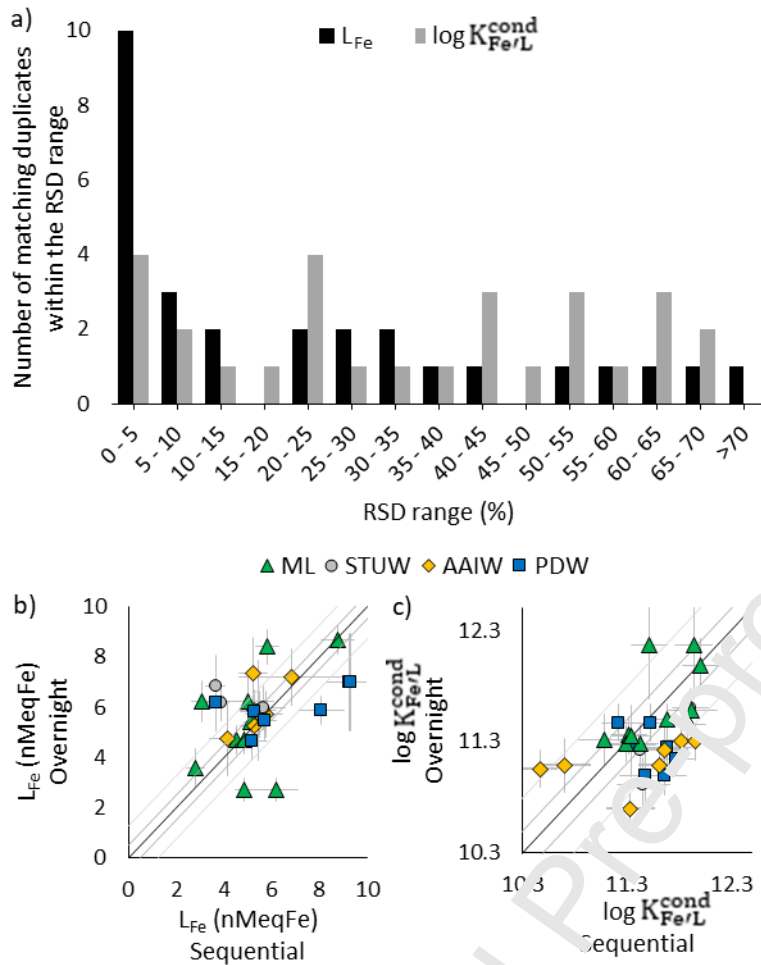


Figure 7. a) Distribution of the RSD of the L_{Fe} and $\log K_{Fe/L}^{cond}$ values and 1:1 plots for b) L_{Fe} and c) $\log K_{Fe/L}^{cond}$ of duplicate titration performed with overnight and sequential equilibration. For the 1:1 plots, the results are shown in function of the water masses, namely the Mixed Layer (ML; green triangles), the Subtropical Underwater (STUW; grey circles), the Antarctic Intermediate Water (AAIW; yellow diamonds), and the Pacific Deep Water (PDW; blue squares). The grey lines correspond to 10 and 25% RSD of the main value for all titrations for L_{Fe} (5.1 nMeqFe) and of the range covered by the detection window for $\log K_{Fe/L}^{cond}$ (2).

The equilibration procedures show an agreement within 10% of the RSD for 46% of the comparison for L_{Fe} and 21% for $\log K_{Fe/L}^{cond}$, and an agreement within 25% of the RSD for 60% of L_{Fe} and 43% of $\log K_{Fe/L}^{cond}$. These results attest to a rather good agreement between sequential and overnight equilibration procedure, especially for L_{Fe} . With this comparison, we state that differences with other methods using overnight equilibration cannot be attributed only to the lack of equilibrium using sequential equilibration as stated in recent comparison studies (Ardiningsih et al., 2021; Gerringa et al., 2021).

For $\log K_{\text{Fe/L}}^{\text{cond}}$, higher values are observed for several samples when applying the sequential equilibration (Figure 7c). This was not a systematic observation, but it does suggest the absence of adjunctive mechanism between natural and added ligands for several samples. Because none of the samples collected in the mixed layer showed higher $\log K_{\text{Fe/L}}^{\text{cond}}$ with the sequential equilibration, we suggest that a slower equilibration kinetic might take place between SA and some of the natural Fe-binding sites composing more aged and mineralized DOM compared to the more reactive Fe-binding ligands found in the mixed layer. Rather than discriminating an equilibration procedure, this comparison suggests that the mineralization state of the DOM impacts Fe-binding sites and their association/dissociation kinetic. It would be of utmost interest to carry out more comparative studies on the equilibration kinetic between natural Fe-binding ligands and SA, and to compare them to methods constraining Fe exchange kinetics (e.g., Boiteau and Repeta, 2022).

Conclusion

We present in this paper a suite of recommendations intended to improve and ease the use of SA as an artificial ligand to investigate DFe organic speciation by CLE-AdCSV. The conditioning, voltametric and voltammogram treatment guidelines simplify the application of the SA method for Metrohm™ and BASi systems, and the titration fitting procedure facilitates comparison and integration of results across laboratories. The titration fitting spreadsheet and procedure are newly developed and are open to recommendations from the community. The automated definition of the QF implemented in this work introduces a tool for qualifying the titration quality and improve data comparison between laboratories, and could help improving our understanding of the organic speciation of trace metals at local and global scales if integrated in future work. The interpretation procedure can be modified for the interpretation of organic speciation data regarding any metal and application specificities such as number of aliquots and voltammogram recorded. Essential aspects for the validation of the procedure include tests on the automation of the voltammograms treatment, on the definition of the sensitivity, and on the reproducibility of the analysis on diverse samples and on multiple analyses of a reference seawater.

Our comparison of equilibration procedures (sequential versus overnight) resulted in L_{Fe} and $\log K_{\text{Fe/L}}^{\text{cond}}$ values within 25% RSD for more than half of the samples. The difference between duplicates in the other half appeared to be random and not systematically biased in one direction or another and suggested specific association/dissociation kinetics for different ligand assemblages. This could be the reason for the historical disagreement regarding the equilibration time in previous work (Rue and Bruland, 1995; Buck et al., 2007; Abualhaija and van den Berg, 2014). The impact of the equilibration time on the CLE-AdCSV results may be better constrained with the use of model ligands and novel mass spectrometry approaches to evaluate kinetics of DFe exchange between the natural binding ligands and the added SA (e.g., Boiteau and Repeta, 2022). These equilibration kinetics for DFe against SA could be a way to discriminate different kinds of ligands or binding-sites in natural samples. Such experiments have already been tested but on the time scale of hours to days (Wu and Luther, 1995; Witter and Luther, 1998; Croot and Heller, 2012). Our optimised SA method with shorter deposition time could allow the investigation of the equilibration kinetics on the time scale of minutes to hours, opening a way to further explore FeL association and dissociation kinetics. Ultimately, we also suggest that the DCM composition could explain the differences in the peak intensity of the FeSA_2 reduction as a function of the deposition potential applied. Indeed, the competition for adsorption on the mercury drop between FeSA_2 , surfactant, and/or electroactive DOM could be dependent on the potential applied. Further work should explore the possibility to develop an indirect pseudopolarographic titration of the DOM against SA.

Declaration of competing interest

The authors have no conflicts of interest to declare.

Data availability

The FeL titration interpretations, the custom spreadsheet and the procedures for the use ECDSOft, ProMCC, and the custom spreadsheet are available in SM. The softwares ECDSOft and ProMCC are freely available online (<https://sites.google.com/site/daromasoft>).

Acknowledgment

The work contained in this paper was conducted during a PhD study supported by the Natural Environment Research Council (NERC) EAO (Earth, Atmosphere and Ocean) Doctoral Training Partnership and is funded by NERC whose support is gratefully acknowledged (grant NE/L002469/1). HW and LM acknowledge support from the British Council, Alliance Hubert Curie Programme: “Investigation of the Marine Sources of Iron-binding Ligands (IMIL)” grant (608178297), and the “PHC Alliance” programme, funded by the UK Department for Business, Energy & Industrial Strategy (now DSIT), the French Ministry for Europe and Foreign Affairs, and the French Ministry of Higher Education, Research and Innovation. DO and PS acknowledge support from the Croatian Science Foundation, project: “New methodological approach to biogeochemical studies of trace metal speciation in coastal aquatic ecosystems (MEBTRACE)” (IP-2014-09-7530-MEBTRACE). This work was conducted on samples collected within the frame of the TONGA project (Shallow hydroThermal sOurces of trace elemeNts: potential impacts on biological productivity and the bioloGicAl carbon pump). We warmly thank Cécile Guieu and Sophie Lemerlet, PIs of the TONGA cruise (GEOTRACES GPpr14, November 2019, <https://doi.org/10.17616/18000884>), Chloé Tilliette for providing DFe data, and all the scientists, the captain, and the crew of the R/V L’Atalante for their cooperative work at sea during the TONGA cruise. KNB and LM were supported by the U.S. National Science Foundation awards NSF-OCE 2300915 and NSF OCE 2310573, and SC by NSF-OCE 1829777.

References

- Abualhaija, M.M., van den Berg, C.M.G., 2014. Chemical speciation of iron in seawater using catalytic cathodic stripping voltammetry with ligand competition against salicylaldoxime. *Mar. Chem.* 164, 60–74. <https://doi.org/10.1016/j.marchem.2014.06.005>
- Apte, S.C., Gardner, M.J., Ravenscroft, J.E., 1988. An evaluation of voltammetric titration procedures for the determination of trace metal complexation in natural waters by use of computers simulation. *Anal. Chim. Acta* 212, 1–21. [https://doi.org/10.1016/S0003-2670\(00\)84124-0](https://doi.org/10.1016/S0003-2670(00)84124-0)
- Ardiningsih, I., Zhu, K., Lodeiro, P., Gledhill, M., Reichart, G.-J., Achterberg, E.P., Middag, R., Gerringa, L.J.A., 2021. Iron Speciation in Fram Strait and Over the Northeast Greenland Shelf: An Inter-Comparison Study of Voltammetric Methods. *Front. Mar. Sci.* 7. <https://doi.org/10.3389/fmars.2020.609379>
- Avendaño, L., Gledhill, M., Achterberg, E.P., Rérolle, V.M.C., Schlosser, C., 2016. Influence of Ocean Acidification on the Organic Complexation of Iron and Copper in Northwest European Shelf Seas; a Combined Observational and Model Study. *Front. Mar. Sci.* 3. <https://doi.org/10.3389/fmars.2016.00058>
- Barbeau, K., Rue, E.L., Bruland, K.W., Butler, A., 2001. Photochemical cycling of iron in the surface ocean mediated by microbial iron(III)-binding ligands. *Nature* 413, 409–413. <https://doi.org/10.1038/35096545>

- Boiteau, R.M., Repeta, D.J., 2022. Slow Kinetics of Iron Binding to Marine Ligands in Seawater Measured by Isotope Exchange Liquid Chromatography-Inductively Coupled Plasma Mass Spectrometry. *Environ. Sci. Technol.* 56, 3770–3779. <https://doi.org/10.1021/acs.est.1c06922>
- Boye, M., van den Berg, C.M.G., de Jong, J.T.M., Leach, H., Croot, P., de Baar, H.J.W., 2001. Organic complexation of iron in the Southern Ocean. *Deep Sea Res. Part Oceanogr. Res. Pap.* 48, 1477–1497. [https://doi.org/10.1016/S0967-0637\(00\)00099-6](https://doi.org/10.1016/S0967-0637(00)00099-6)
- Bressac, M., Guieu, C., Ellwood, M.J., Tagliabue, A., Wagener, T., Laurenceau-Cornec, E.C., Whitby, H., Sarthou, G., Boyd, P.W., 2019. Resupply of mesopelagic dissolved iron controlled by particulate iron composition. *Nat. Geosci.* 12, 995–1000. <https://doi.org/10.1038/s41561-019-0476-6>
- Buck, K.N., Gerringa, L.J.A., Rijkenberg, M.J.A., 2016. An Intercomparison of Dissolved Iron Speciation at the Bermuda Atlantic Time-series Study (BATS) Site: Results from GEOTRACES Crossover Station A. *Front. Mar. Sci.* 3, UNSP 262. <https://doi.org/10.3389/fmars.2016.00262>
- Buck, K.N., Lohan, M.C., Berger, C.J.M., Bruland, K.W., 2007. Dissolved iron speciation in two distinct river plumes and an estuary: Implications for riverine iron supply. *Limnol. Oceanogr.* 52, 843–855. <https://doi.org/10.4319/lo.2007.52.2.0843>
- Buck, K.N., Moffett, J., Barbeau, K.A., Bundy, R.M., Kondo, Y., Wu, J., 2012. The organic complexation of iron and copper: an intercomparison of competitive ligand exchange-adsorptive cathodic stripping voltammetry (CLE-CSV) techniques. *Limnol. Oceanogr. Methods* 10, 496–515. <https://doi.org/10.4319/lom.2012.10.496>
- Buck, K.N., Sedwick, P.N., Sohst, B., Carlson, C.A., 2018. Organic complexation of iron in the eastern tropical South Pacific: Results from US GEOTRACES Eastern Pacific Zonal Transect (GEOTRACES cruise GP16). *Mar. Chem., The U.S. GEOTRACES Eastern Tropical Pacific Transect (GP16)* 201, 229–241. <https://doi.org/10.1016/j.marchem.2017.11.007>
- Buck, K.N., Selph, K.E., Barbeau, K.A., 2010. Iron-binding ligand production and copper speciation in an incubation experiment of Arctic Peninsula shelf waters from the Bransfield Strait, Southern Ocean. *Mar. Chem.* 122, 148–159. <https://doi.org/10.1016/j.marchem.2010.06.002>
- Buck, K.N., Sohst, B., Sedwick, P.N., 2015. The organic complexation of dissolved iron along the U.S. GEOTRACES (GA03) North Atlantic Section. *Deep Sea Res. Part II Top. Stud. Oceanogr.* 116, 152–165. <https://doi.org/10.1016/j.dsr2.2014.11.016>
- Bundy, R.M., Abdulla, H.A.N., Harner, P.G., Biller, D.V., Buck, K.N., Barbeau, K.A., 2015. Iron-binding ligands and humic substances in the San Francisco Bay estuary and estuarine-influenced shelf regions of coastal California. *Mar. Chem., SCOR WG 139: Organic Ligands – A Key Control on Trace Metal Biogeochemistry in the Ocean* 173, 183–194. <https://doi.org/10.1016/j.marchem.2014.11.005>
- Bundy, R.M., Biller, D.V., Buck, K.N., Bruland, K.W., Barbeau, K.A., 2014. Distinct pools of dissolved iron-binding ligands in the surface and benthic boundary layer of the California Current. *Limnol. Oceanogr.* 59, 769–787. <https://doi.org/10.4319/lo.2014.59.3.0769>
- Bundy, R.M., Boiteau, R.M., McLean, C., Turk-Kubo, K.A., McIlvin, M.R., Saito, M.A., Van Mooy, B.A.S., Repeta, D.J., 2018. Distinct Siderophores Contribute to Iron Cycling in the Mesopelagic at Station ALOHA. *Front. Mar. Sci.* 5. <https://doi.org/10.3389/fmars.2018.00061>
- Cabanes, D.J.E., Norman, L., Bowie, A.R., Strmečki, S., Hassler, C.S., 2020. Electrochemical evaluation of iron-binding ligands along the Australian GEOTRACES southwestern Pacific section (GP13). *Mar. Chem.* 219, 103736. <https://doi.org/10.1016/j.marchem.2019.103736>
- Chapman, C.S., van den Berg, C.M.G., 2007. Anodic Stripping Voltammetry Using a Vibrating Electrode. *Electroanalysis* 19, 1347–1355. <https://doi.org/10.1002/elan.200703873>
- Cobelo-García, A., Santos-Echeandía, J., López-Sánchez, D.E., Almécija, C., Omanović, D., 2014. Improving the Voltammetric Quantification of Ill-Defined Peaks Using Second Derivative Signal Transformation: Example of the Determination of Platinum in Water and Sediments. *Anal. Chem.* 86, 2308–2313. <https://doi.org/10.1021/ac403558y>
- Croot, P.L., Johansson, M., 2000. Determination of Iron Speciation by Cathodic Stripping Voltammetry in Seawater Using the Competing Ligand 2-(2-Thiazolylazo)-p-cresol (TAC). *Electroanalysis* 12, 565–576. [https://doi.org/10.1002/\(SICI\)1521-4109\(200005\)12:8<565::AID-ELAN565>3.0.CO;2-L](https://doi.org/10.1002/(SICI)1521-4109(200005)12:8<565::AID-ELAN565>3.0.CO;2-L)

- Croot, P.L., Heller, M.I., 2012. The Importance of Kinetics and Redox in the Biogeochemical Cycling of Iron in the Surface Ocean. *Front. Microbiol.* 3. <https://doi.org/10.3389/fmicb.2012.00219>
- Donat, J.R., Bruland, K.W., 1988. Direct determination of dissolved cobalt and nickel in seawater by differential pulse cathodic stripping voltametry preceded by adsorptive collection of cyclohexane-1,2-dione dioxime complexes. *Anal Chem U. S.* 60:3. <https://doi.org/10.1021/ac00154a011>
- Dulaquais, G., Fourrier, P., Guieu, C., Mahieu, L., Riso, R., Salaun, P., Tilliette, C., Whitby, H., 2023. The role of humic-type ligands in the bioavailability and stabilization of dissolved iron in the Western Tropical South Pacific Ocean. *Front. Mar. Sci.* 10. <https://doi.org/10.3389/fmars.2023.1219594>
- Fonvielle, J.A., Felgate, S.L., Tanentzap, A.J., Hawkes, J.A., 2023. Assessment of sample freezing as a preservation technique for analysing the molecular composition of dissolved organic matter in aquatic systems. *RSC Adv.* 13, 24594–24603. <https://doi.org/10.1039/D3RA01349A>
- Fourrier, P., Dulaquais, G., Guigue, C., Giamarchi, P., Sarthou, G., Whitby, H., Riso, R., 2022. Characterization of the vertical size distribution, composition and chemical properties of dissolved organic matter in the (ultra)oligotrophic Pacific Ocean through a multi-detection approach. *Mar. Chem.* 240, 104068. <https://doi.org/10.1016/j.marchem.2021.104068>
- Fourrier, Pierre, Dulaquais, G., Riso, R., 2022. Influence of the conservation mode of seawater for dissolved organic carbon analysis. *Mar. Environ. Res.* 181, 105754. <https://doi.org/10.1016/j.marenvres.2022.105754>
- Garnier, C., Pižeta, I., Mounier, S., Benaïm, J.Y., Branica, M., 2004. Influence of the type of titration and of data treatment methods on metal complexing parameters determination of single and multi-ligand systems measured by stripping voltammetry. *Anal. Chim. Acta* 505, 263–275. <https://doi.org/10.1016/j.aca.2003.10.066>
- Gerringa, L.J.A., Gledhill, M., Ardiningsih, I., Moutje, N., Laglera, L.M., 2021. Comparing CLE-AdCSV applications using SA and TAC to determine the Fe-binding characteristics of model ligands in seawater. *Biogeosciences* 18, 5265–5289. <https://doi.org/10.5194/bg-18-5265-2021>
- Gerringa, L.J.A., Herman, P.M.J., Poortvliet, T.C.W., 1995. Comparison of the linear Van den Berg/Ružić transformation and a non-linear fit of the Langmuir isotherm applied to Cu speciation data in the estuarine environment. *Mar. Chem.* 48, 131–142. [https://doi.org/10.1016/0304-4203\(94\)00041-B](https://doi.org/10.1016/0304-4203(94)00041-B)
- Gerringa, L.J.A., Rijkenberg, M.J.A., Thuróczy, C.-E., Maas, L.R.M., 2014. A critical look at the calculation of the binding characteristics and concentration of iron complexing ligands in seawater with suggested improvements. *Environ. Chem.* 11, 114–136. <https://doi.org/10.1071/EN13072>
- Gledhill, M., Achterberg, F.P., Li, K., Mohamed, K.N., Rijkenberg, M.J.A., 2015. Influence of ocean acidification on the complexation of iron and copper by organic ligands in estuarine waters. *Mar. Chem., Cycles of metals and carbon in the oceans - A tribute to the work stimulated by Hein de Baar* 177, 421–433. <https://doi.org/10.1016/j.marchem.2015.03.016>
- Gledhill, M., Buck, K.N., 2012. The Organic Complexation of Iron in the Marine Environment: A Review. *Front. Microbiol.* 3. <https://doi.org/10.3389/fmicb.2012.00069>
- Gledhill, M., van den Berg, C.M.G., 1994. Determination of complexation of iron(III) with natural organic complexing ligands in seawater using cathodic stripping voltammetry. *Mar. Chem.* 47, 41–54. [https://doi.org/10.1016/0304-4203\(94\)90012-4](https://doi.org/10.1016/0304-4203(94)90012-4)
- Gourain, A., 2020. Copper biogeochemical cycle and the organic complexation of dissolved copper in the North Atlantic (phd). University of Liverpool.
- Guieu, C., Bonnet, S., 2019. TONGA 2019 cruise, L'Atalante R/V. <https://doi.org/10.17600/18000884>
- Gupta, B.S., Taha, M., Lee, M.-J., 2013. Stability Constants for the Equilibrium Models of Iron(III) with Several Biological Buffers in Aqueous Solutions. *J. Solut. Chem.* 42, 2296–2309. <https://doi.org/10.1007/s10953-013-0107-6>
- Hassler, C., Cabanes, D., Blanco-Ameijeiras, S., Sander, S.G., Benner, R., Hassler, C., Cabanes, D., Blanco-Ameijeiras, S., Sander, S.G., Benner, R., 2019. Importance of refractory ligands and their photodegradation for iron oceanic inventories and cycling. *Mar. Freshw. Res.* 71, 311–320. <https://doi.org/10.1071/MF19213>

- Hassler, C.S., Berg, V.D., G, C.M., Boyd, P.W., 2017. Toward a Regional Classification to Provide a More Inclusive Examination of the Ocean Biogeochemistry of Iron-Binding Ligands. *Front. Mar. Sci.* 4. <https://doi.org/10.3389/fmars.2017.00019>
- Hassler, C.S., Norman, L., Mancuso Nichols, C.A., Clementson, L.A., Robinson, C., Schoemann, V., Watson, R.J., Doblin, M.A., 2015. Iron associated with exopolymeric substances is highly bioavailable to oceanic phytoplankton. *Mar. Chem., SCOR WG 139: Organic Ligands – A Key Control on Trace Metal Biogeochemistry in the Ocean* 173, 136–147. <https://doi.org/10.1016/j.marchem.2014.10.002>
- Hassler, C.S., Schoemann, V., Nichols, C.M., Butler, E.C.V., Boyd, P.W., 2011. Saccharides enhance iron bioavailability to Southern Ocean phytoplankton. *Proc. Natl. Acad. Sci.* 108, 1076–1081. <https://doi.org/10.1073/pnas.1010963108>
- Heller, M., Gaiero, D., Croot, P., 2013. Basin scale survey of marine humic fluorescence in the Atlantic: Relationship to iron solubility and H₂O₂. *Glob. Biogeochem. Cycles* 27. <https://doi.org/10.1029/2012GB004427>
- Ibisanmi, E., Sander, S.G., Boyd, P.W., Bowie, A.R., Hunter, K.A., 2011. Vertical distributions of iron(III) complexing ligands in the Southern Ocean. *Deep Sea Res. Part II Top. Stud. Oceanogr., Biogeochemistry of the Australian Sector of the Southern Ocean* 58, 2113–2125. <https://doi.org/10.1016/j.dsr2.2011.05.028>
- Kleint, C., Zitoun, R., Neuholz, R., Walter, M., Schnetger, B., Kloss, L., Chiswell, S.M., Middag, R., Laan, P., Sander, S.G., Koschinsky, A., 2022. Trace Metal Dynamics in Shallow Hydrothermal Plumes at the Kermadec Arc. *Front. Mar. Sci.* 8. <https://doi.org/10.3389/fmars.2022.895454>
- Laglera, L.M., Battaglia, G., van den Berg, C.M.G., 2011. Effect of humic substances on the iron speciation in natural waters by CLE-AdCSV. *Mar. Chem.* 127, 134–143. <https://doi.org/10.1016/j.marchem.2011.09.005>
- Laglera, L.M., Downes, J., Santos-Echeandía, J., 2013. Comparison and combined use of linear and non-linear fitting for the estimation of complexing parameters from metal titrations of estuarine samples by CLE/AdCSV. *Mar. Chem.* 155, 102–112. <https://doi.org/10.1016/j.marchem.2013.06.005>
- Laglera, L.M., Filella, M., 2015. The relevance of ligand exchange kinetics in the measurement of iron speciation by CLE-AdCSV in seawater. *Mar. Chem., SCOR WG 139: Organic Ligands – A Key Control on Trace Metal Biogeochemistry in the Ocean* 173, 100–113. <https://doi.org/10.1016/j.marchem.2014.09.005>
- Liu, X., Millero, F.J., 2002. The solubility of iron in seawater. *Mar. Chem.* 77, 43–54. [https://doi.org/10.1016/S0304-4203\(01\)00074-3](https://doi.org/10.1016/S0304-4203(01)00074-3)
- Lodeiro, P., Rey-Castro, C., David, C., Achterberg, E.P., Puy, J., Gledhill, M., 2020. Acid-base properties of dissolved organic matter extracted from the marine environment. *Sci. Total Environ.* 729, 138–137. <https://doi.org/10.1016/j.scitotenv.2020.138437>
- Louis, Y., Cmuk, P., Omanović, D., Garnier, C., Lenoble, V., Mounier, S., Pižeta, I., 2008. Speciation of trace metals in natural waters: The influence of an adsorbed layer of natural organic matter (NOM) on voltammetric behaviour of copper. *Anal. Chim. Acta* 606, 37–44. <https://doi.org/10.1016/j.aca.2007.11.011>
- Louis, Y., Garnier, C., Lenoble, V., Omanović, D., Mounier, S., Pižeta, I., 2009. Characterisation and modelling of marine dissolved organic matter interactions with major and trace cations. *Mar. Environ. Res.* 67, 100–107. <https://doi.org/10.1016/j.marenvres.2008.12.002>
- Mahieu, L., 2023. Analytical challenges, development and application of CLE-ACSV for the determination of the organic speciation of iron in marine waters (phd). University of Liverpool.
- Miller, L.A., Bruland, K.W., 1997. Competitive equilibration techniques for determining transition metal speciation in natural waters: Evaluation using model data. *Anal. Chim. Acta* 343, 161–181. [https://doi.org/10.1016/S0003-2670\(96\)00565-X](https://doi.org/10.1016/S0003-2670(96)00565-X)
- Millero, F.J., Zhang, J.-Z., Fiol, S., Sotolongo, S., Roy, R.N., Lee, K., Mane, S., 1993. The use of buffers to measure the pH of seawater. *Mar. Chem.* 44, 143–152. [https://doi.org/10.1016/0304-4203\(93\)90199-X](https://doi.org/10.1016/0304-4203(93)90199-X)
- Moore, C.M., Mills, M.M., Arrigo, K.R., Berman-Frank, I., Bopp, L., Boyd, P.W., Galbraith, E.D., Geider, R.J., Guieu, C., Jaccard, S.L., Jickells, T.D., La Roche, J., Lenton, T.M., Mahowald,

- N.M., Marañón, E., Marinov, I., Moore, J.K., Nakatsuka, T., Oschlies, A., Saito, M.A., Thingstad, T.F., Tsuda, A., Ulloa, O., 2013. Processes and patterns of oceanic nutrient limitation. *Nat. Geosci.* 6, 701–710. <https://www.nature.com/articles/ngeo1765>
- Morel, F.M.M., Price, N.M., 2003. The Biogeochemical Cycles of Trace Metals in the Oceans. *Science* 300, 944–947. <https://doi.org/10.1126/science.1083545>
- Norman, L., Worms, I.A.M., Angles, E., Bowie, A.R., Nichols, C.M., Ninh Pham, A., Slaveykova, V.I., Townsend, A.T., David Waite, T., Hassler, C.S., 2015. The role of bacterial and algal exopolymeric substances in iron chemistry. *Mar. Chem., SCOR WG 139: Organic Ligands – A Key Control on Trace Metal Biogeochemistry in the Ocean* 173, 148–161. <https://doi.org/10.1016/j.marchem.2015.03.015>
- Omanović, D., Garnier, C., Louis, Y., Lenoble, V., Mounier, S., Pižeta, I., 2010. Significance of data treatment and experimental setup on the determination of copper complexing parameters by anodic stripping voltammetry. *Anal. Chim. Acta* 664, 136–143. <https://doi.org/10.1016/j.aca.2010.02.008>
- Omanović, D., Garnier, C., Pižeta, I., 2015. ProMCC: An all-in-one tool for trace metal complexation studies. *Mar. Chem., SCOR WG 139: Organic Ligands – A Key Control on Trace Metal Biogeochemistry in the Ocean* 173, 25–39. <https://doi.org/10.1016/j.marchem.2014.10.011>
- Pižeta, I., Sander, S.G., Hudson, R.J.M., Omanović, D., Baars, O., Bourbon, K.A., Buck, K.N., Bundy, R.M., Carrasco, G., Croot, P.L., Garnier, C., Gerringa, L.J.A., Gledhill, M., Hirose, K., Kondo, Y., Laglera, L.M., Nuester, J., Rijkenberg, M.J.A., Takeda, S., Twining, B.S., Wells, M., 2015. Interpretation of complexometric titration data: An intercomparison of methods for estimating models of trace metal complexation by natural organic ligands. *Mar. Chem., SCOR WG 139: Organic Ligands – A Key Control on Trace Metal Biogeochemistry in the Ocean* 173, 3–24. <https://doi.org/10.1016/j.marchem.2015.03.006>
- Rue, E.L., Bruland, K.W., 1995. Complexation of iron(III) by natural organic ligands in the Central North Pacific as determined by a new competitive ligand equilibration/adsorptive cathodic stripping voltammetric method. *Mar. Chem., The Chemistry of Iron in Seawater and its Interaction with Phytoplankton* 50, 117–138. [https://doi.org/10.1016/0304-4203\(95\)00031-L](https://doi.org/10.1016/0304-4203(95)00031-L)
- Ružić, I., 1982. Theoretical aspects of the direct titration of natural waters and its information yield for trace metal speciation. *Anal. Chim. Acta* 140, 99–113. [https://doi.org/10.1016/S0003-2670\(01\)95456-X](https://doi.org/10.1016/S0003-2670(01)95456-X)
- Salaün, P., Planer-Friedrich, B., van den Berg, C.M.G., 2007. Inorganic arsenic speciation in water and seawater by anodic stripping voltammetry with a gold microelectrode. *Anal. Chim. Acta* 585, 312–322. <https://doi.org/10.1016/j.aca.2006.12.048>
- Sander, S.G., Hunter, K.A., Harris, H., Wells, M., 2011. Numerical Approach to Speciation and Estimation of Parameters Used in Modeling Trace Metal Bioavailability. *Environ. Sci. Technol.* 45, 6388–6397. <https://doi.org/10.1021/es200113v>
- Sanvito, F., Monticelli, D., 2020. Fast iron speciation in seawater by catalytic Competitive Ligand Equilibration-Cathodic Stripping Voltammetry with tenfold sample size reduction. *Anal. Chim. Acta* 1113, 9–17. <https://doi.org/10.1016/j.aca.2020.04.002>
- Sanvito, F., Pacileo, L., Monticelli, D., 2019. Fostering and Understanding Iron Detection at the Ultratrace Level by Adsorptive Stripping Voltammetry with Catalytic Enhancement. *Electroanalysis* 31, 212–216. <https://doi.org/10.1002/elan.201800675>
- Scatchard, G., 1949. The Attractions of Proteins for Small Molecules and Ions. *Ann. N. Y. Acad. Sci.* 51, 660–672. <https://doi.org/10.1111/j.1749-6632.1949.tb27297.x>
- Slagter, H.A., Laglera, L.M., Sukekava, C., Gerringa, L.J.A., 2019. Fe-Binding Organic Ligands in the Humic-Rich TransPolar Drift in the Surface Arctic Ocean Using Multiple Voltammetric Methods. *J. Geophys. Res. Oceans* 124, 1491–1508. <https://doi.org/10.1029/2018JC014576>
- Tilliette, C., Taillandier, V., Bouruet-Aubertot, P., Grima, N., Maes, C., Montanes, M., Sarthou, G., Vorrath, M.-E., Arnone, V., Bressac, M., González-Santana, D., Gazeau, F., Guieu, C., 2022. Dissolved Iron Patterns Impacted by Shallow Hydrothermal Sources Along a Transect Through the Tonga-Kermadec Arc. *Glob. Biogeochem. Cycles* 36, e2022GB007363. <https://doi.org/10.1029/2022GB007363>
- Twining, B.S., Baines, S.B., 2013. The Trace Metal Composition of Marine Phytoplankton. *Annu. Rev. Mar. Sci.* 5, 191–215. <https://doi.org/10.1146/annurev-marine-121211-172322>

- van den Berg, C.M.G., 2006. Chemical Speciation of Iron in Seawater by Cathodic Stripping Voltammetry with Dihydroxynaphthalene. *Anal. Chem.* 78, 156–163. <https://doi.org/10.1021/ac051441+>
- van den Berg, C.M.G., 1995. Evidence for organic complexation of iron in seawater. *Mar. Chem., The Chemistry of Iron in Seawater and its Interaction with Phytoplankton* 50, 139–157. [https://doi.org/10.1016/0304-4203\(95\)00032-M](https://doi.org/10.1016/0304-4203(95)00032-M)
- van den Berg, C.M.G., 1982. Determination of copper complexation with natural organic ligands in seawater by equilibration with MnO₂ II. Experimental procedures and application to surface seawater. *Mar. Chem.* 11, 323–342. [https://doi.org/10.1016/0304-4203\(82\)90029-9](https://doi.org/10.1016/0304-4203(82)90029-9)
- van den Berg, C.M.G., Donat, J.R., 1992. Determination and data evaluation of copper complexation by organic ligands in sea water using cathodic stripping voltammetry at varying detection windows. *Anal. Chim. Acta* 257, 281–291. [https://doi.org/10.1016/0003-2670\(92\)85181-5](https://doi.org/10.1016/0003-2670(92)85181-5)
- Wang, P., Ding, Y., Liang, Y., Liu, M., Lin, X., Ye, Q., Shi, Z., 2021. Linking molecular composition to proton and copper binding ability of fulvic acid: A theoretical modeling approach based on FT-ICR-MS analysis. *Geochim. Cosmochim. Acta* 312, 279–298. <https://doi.org/10.1016/j.gca.2021.07.019>
- Whitby, H., Bressac, M., Sarthou, G., Ellwood, M.J., Guieu, C., Foya, P.W., 2020a. Contribution of Electroactive Humic Substances to the Iron-Binding Ligands Released During Microbial Remineralization of Sinking Particles. *Geophys. Res. Lett.* 47, e2019GL086685. <https://doi.org/10.1029/2019GL086685>
- Whitby, H., Planquette, H., Cassar, N., Bucciarelli, E., Cabun, C.L., Janssen, D.J., Cullen, J.T., González, A.G., Völker, C., Sarthou, G., 2020b. A call for refining the role of humic-like substances in the oceanic iron cycle. *Sci. Rep.* 10, 1–12. <https://doi.org/10.1038/s41598-020-62266-7>
- Whitby, H., Posacka, A.M., Maldonado, M.T., van den Berg, C.M.G., 2018. Copper-binding ligands in the NE Pacific. *Mar. Chem.* 204, 36–48. <https://doi.org/10.1016/j.marchem.2018.05.008>
- Witter, A.E., Luther, G.W., 1998. Variation in Fe-organic complexation with depth in the Northwestern Atlantic Ocean as determined using a kinetic approach. *Mar. Chem.* 62, 241–258. [https://doi.org/10.1016/S0304-4203\(98\)00044-9](https://doi.org/10.1016/S0304-4203(98)00044-9)
- Wu, J., Luther, G.W., 1995. Complexation of Fe(III) by natural organic ligands in the Northwest Atlantic Ocean by a competitive ligand equilibration method and a kinetic approach. *Mar. Chem., The Chemistry of Iron in Seawater and its Interaction with Phytoplankton* 50, 159–177. [https://doi.org/10.1016/0304-4203\(95\)00033-N](https://doi.org/10.1016/0304-4203(95)00033-N)
- Yokoi, K., van den Berg, C.M.G., 1992. The determination of iron in seawater using catalytic cathodic stripping voltammetry. *Electroanalysis* 4, 65–69. <https://doi.org/10.1002/elan.1140040113>